O-GlcNAcylation of orphan nuclear receptor ERRγ promotes hepatic gluconeogenesis

Running title: *O*-GlcNAcylation of ERRγ

Jagannath Misra[1], Don-Kyu Kim[1], Yoon Seok Jung[1], Han Byeol Kim[2], Yong-Hoon Kim[3], Eun-Kyung Yoo[4], Byung Gyu Kim[5], Sunghoon Kim[6], In-Kyu Lee[4], Robert A. Harris[7], Jeong-Sun Kim[8], Chul-Ho Lee[3], Jin Won Cho[2] and Hueng-Sik Choi[1]*

[1]National Creative Research Initiatives Center for Nuclear Receptor Signals and Hormone Research Center, School of Biological Sciences and Technology, Chonnam National University, Gwangju 500-757, Republic of Korea. [2]Department of Integrated OMICS for Biomedical Science, Yonsei University, Seoul 120-749, Republic of Korea. [3]Korea Research Institute of Bioscience and Biotechnology, Daejeon 305-806, Republic of Korea. [4]Department of Internal Medicine, Kyungpook National University School of Medicine, Deagu 700-721, Republic of Korea. [5]Leading-edge Research Center for Drug Discovery and Development and Metabolic Disease, Kyungpook National University, Daegu 700-721, Korea. [6]Medicinal Bioconvergence Research Center Department of Molecular Medicine and Biopharmaceutical Sciences Graduate School of Convergence Science and Technology College of Pharmacy, Seoul National University, Seoul 151-742, Korea. [7]Department of Biochemistry and Molecular Biology, Indiana University School of Medicine and the Roudebush VA Medical Center, Indianapolis, Indiana 46202, United States of America. [8]Department of Chemistry and Institute of Basic Sciences, Chonnam National University, Gwangju 500-757, Republic of Korea.

Diabetes Publish Ahead of Print, published online June 22, 2016

*Address correspondence to:

Hueng-Sik Choi

National Creative Research Initiatives Center for Nuclear Receptor Signals and Hormone Research Center, School of Biological Sciences and Technology, Chonnam National University, Gwangju 500-757, Republic of Korea. Tel.: +82-62-530-0506; Fax: +82-62-530-0506; E-mail: hsc@chonnam.ac.kr.

This manuscript contains 5,571 words, 6 figures and 4 supplementary figures.

ABSTRACT

Estrogen-related receptor γ (ERRγ) is a major positive regulator of hepatic gluconeogenesis. Its transcriptional activity is suppressed by phosphorylation signaled by insulin in the fed state, but whether post-translational modification (PTM) alters its gluconeogenic activity in the fasted state is not known. Metabolically active hepatocytes direct a small amount of glucose into the hexosamine biosynthetic pathway (HBP) leading to protein *O*-GlcNAcylation. Here we demonstrate that ERRγ is *O*-GlcNAcylated by *O*-GlcNAc transferase (OGT) in the fasted state. This stabilizes the protein by inhibiting proteasome mediated protein degradation, increasing ERRγ recruitment to gluconeogenic gene promoters. Mass spectrometry identifies two serine residues (S317, S319) present in the ERRγ ligand binding domain (LBD) that are *O*-GlcNAcylated. Mutation of these residues destabilizes ERRγ protein, and blocks the ability of ERRγ to induce gluconeogenesis *in vivo*. The impact of this pathway on gluconeogenesis *in vivo* was confirmed by the observation that decreasing the amount of *O*-GlcNAcylated ERRγ by overexpressing the deglycosylating enzyme *O*-GlcNAcase (OGA) decreases ERRγ dependent glucose production in fasted mice. We conclude that *O*-GlcNAcylation of ERRγ serves as a major signal to promote hepatic gluconeogenesis.

INTRODUCTION

O-GlcNAcylation works as a nutrient sensor in the liver to maintain energy homeostasis in response to varying nutrient flux [1]. *O*-GlcNAcylation is extensively linked with glucose metabolism in liver. L-glutamine fructose-6-phosphate amidotransferase (GFAT) overexpression leads to peripheral insulin resistance [2], [3]. Transgenic mice overexpressing OGT in skeletal muscle and fat exhibit elevated circulating insulin levels and insulin resistance [4]. IRS1/IRS2 of insulin signaling is *O*-GlcNAcylated [5], and *O*-GlcNAcylation has been shown to be a negative regulator of insulin signaling [6]. *O*-GlcNAcylation of FOXO1, CRTC2 and PGC-1α modulates expression of gluconeogenic genes [7], [8], [9], [10]. Chronic increase in *O*-GlcNAcylation levels of PDX1 and NeuroD1 may contribute to hyperinsulinemia in Type 2 diabetes [11], [12]. Thus, by being intimately intertwined with metabolism, HBP and its end product *O*-GlcNAc link transcriptional processes to cellular glucose metabolism and insulin resistance.

Estrogen-related receptors (ERRs) are members of the NR3B subfamily of nuclear receptors, which include ERRα, ERRβ and ERRγ. ERRγ is primarily expressed in heart, brain, kidney, pancreas and liver tissues and is induced during fasting in murine liver [13], [14], [15]. ERRγ plays an important role in the regulation of glucose, lipid, alcohol and iron metabolism in mouse liver [16], [17]. Hepatic ERRγ expression is induced in fasting and the diabetic state, and causes insulin resistance and glucose intolerance [18]. Induction of hepatic ERRγ impairs insulin signaling through diacylglycerol-mediated protein kinase ε activation [19], suggesting that ERRγ transcriptional activity could be involved in insulin action to maintain glucose homeostasis. Recently our laboratory reported that insulin-dependent phosphorylation of ERRγ alters its transcriptional activity to suppress hepatic gluconeogenesis in the fed state [20].

PGC-1α is a transcriptional co-activator involved in hepatic glucose metabolism. Fasting induces hepatic PGC-1α expression that directly interacts with transcription factors including HNF4α, FOXO1, and GR to increase the expression of gluconeogenic genes [21] [22]. PGC-1α overexpression leads to increased expression of G6Pase and PEPCK, key enzymes in the hepatic gluconeogenesis. Conversely, knockdown or knockout of PGC-1α results in lower blood glucose levels as a result of reduced gluconeogenesis.

As insulin-dependent PTM regulates the transcriptional activity of ERRγ in the fed state, herein we investigated whether fasting-dependent activation of the transcriptional activity of ERRγ involves *O*-GlcNAcylation. We demonstrate that the fasting condition triggers *O*-GlcNAcylation of ERRγ that results in protein stabilization. *O*-GlcNAcylation of ERRγ by OGT decreases its ubiquitination (Ub), and cooperatively upregulates gluconeogenesis. In contrast, the fed condition decreases *O*-GlcNAcylation of ERRγ, resulting in ubiquitin-mediated protein degradation. Overall, our study describes how *O*-GlcNAcylation modulates gluconeogenesis via ERRγ.

RESEARCH DESIGN AND METHODS

Animal Experiments

Male 8-week-old C57BL/6J mice, maintained at the Korea Research Institute of Bioscience and Biotechnology (KRIBB) were fed either a high fat diet (HFD) (D12492; Research Diets, New Brunswick, NJ) or a normal chow diet for 12 weeks. At the end of 12 weeks mice were sacrificed and liver tissue was utilized for identification of *O*-GlcNAcylation of ERRγ. *ob*/*ob* and *db*/*db* mice (7–12 weeks old; Charles River Laboratories) were maintained at KRIBB in an animal facility with *ad libitum* access to water and a standard laboratory diet. Liver tissue was utilized for identification of *O*-GlcNAcylation of ERRγ. Male 7-week old C57BL/6J mice (The Jackson Laboratory, Bar Harbor, Maine, USA) were obtained from Ochang Branch Institute, KRIBB. After two weeks, adenoviruses (Ad-GFP, Ad-wt ERRγ and Ad-Ser317Ala+Ser319Ala ERRγ; 5.9 x 10^9 plaque-forming units/mouse) were delivered by tail-vein injection into mice. Glucose tolerance test was performed at day 5 after a tail-vein injection of adenoviruses. Briefly, mice fasted 16 h were injected intraperitoneally with 1 g/kg glucose, and blood glucose was measured in tail-vein blood using a blood glucose meter and test trips (Accu-Chek Aviva meter system; Roche Diagnostics, Indianapolis, IN, USA). All mice were acclimatized to a 12 h light-dark cycle at 22±2^{0}C with free access to food and water in a specific pathogen-free facility. All animal experiments were approved and performed by the Institutional Animal Care and Use Committee of KRIBB.

Glucose Output Assay

Glucose production from primary mouse hepatocytes was measured using a colorimetric glucose oxidase assay kit according to the manufacturer's protocol. Briefly, after the

experimental time period as indicated, the cells were washed three times with phosphate-buffered saline. Then the cells were incubated for 3 h at 37 °C, 5% CO_2, in glucose production buffer (glucose-free DMEM, pH 7.4, containing 20 mmol/liter sodium lactate, 1 mmol/liter sodium pyruvate, and 15 mmol/liter HEPES, without phenol red), and the glucose assays were performed.

Glucagon Assay

Blood glucagon levels were measured using mouse glucagon EIA kit (Ray Biotech, Inc.) following manufacturer's protocol.

Cell culture and reagents

Primary hepatocytes were isolated from C57BL/6J mice (male, 20-30 g) by collagenase perfusion [23] and seeded with Medium 199 (Cellgro). After 3–6 h of attachment, cells were infected with the indicated adenoviruses for overexpression or treated with various chemicals as indicated. HEK 293T and AML12 cells were maintained as described previously [24]. Transient transfection was performed using Lipofectamine 2000 (Invitrogen) or SuperFect (Qiagen, Hilden, Germany) according to the manufacturers' instructions. β-N-Acetyl-D-glucosamine (GlcN), 6-diazo-5-oxo-L-norleucine (DON), glucagon, insulin, cycloheximide (CHX), ANTI-FLAG M2 affinity gel, glucose oxidase assay kit and streptozotocin (STZ) were purchased from SIGMA. MG-132 protease inhibitors were purchased from Calbiochem. Express Protein Labeling Mix [^{35}S] (NEG072002MC) was purchased from Perkin Elmer. Mouse Glucagon EIA kit (EIAM-GLU) was purchased from Ray Biotech, Inc. Antibodies were purchased as follows : *O*-GlcNAc from Covance, α-tubulin from Abfrontier, ERRγ from Perseus Proteomix, OGT from

Abcam, FLAG, Anti-FLAG M2 and HA from Cell Signaling, and G6Pase, Mdm2, ubiquitin, Gal4, PGC-1α and PEPCK from Santa Cruz Biotechnology.

Plasmid and adenovirus vector constructs

Expression vectors for HA-ERRγ, FLAG-ERRγ, HA-PGC-1α and Sft4-luc containing three copies of the ERRγ binding site were described previously [25]. HA-ERRα was described previously [26]. FLAG-human OGT was constructed by inserting the full PCR fragment of the open reading frame into the Not1/Sal1 sites of the p3XFLAG-CMV-7.1 vector. FLAG-human OGA was constructed by inserting the full PCR fragment of the open reading frame into the Bgl2/Sal1 sites of the pFLAG-CMV-7.1 vector. FLAG-mutant ERRγ's (Ser317Ala, Ser319Ala, Ser317Ala+Ser319Ala) were constructed using wild-type ERRγ as template by Quick Change Lightning Site-Directed Mutagenesis kit from Agilent Technologies. Gal4-DBD and Gal4-tk-Luc were described previously [27]. Briefly, Gal4-ERRγ-LBD is a fusion protein consisting of the Gal4 DNA binding domain (Gal4-DBD; amino acids 1–147) and ERRγ ligand binding domain (ERRγ-LBD; amino acids 189–458). This fusion protein activates transcription of a reporter construct (Gal4-tk-luc) containing five GAL4 binding sites (upstream activator sequence) upstream of the firefly luciferase gene in the pGL2-Promoter. Gal4-DBD-Ser317Ala ERRγ, Gal4-DBD-Ser319Ala ERRγ, and Gal4-DBD-Ser317Ala+Ser319Ala ERRγ were constructed using Gal4-DBD-wild-type ERRγ as template by Quick Change Lightning Site-Directed Mutagenesis kit from Agilent Technologies. wtPEPCK-luc, and ERRE mutant PEPCK-luc were described previously [28]. Adenoviruses expressing unspecific (US) shRNA, shERRγ, control GFP, and ERRγ were described previously [28]. Adenovirus OGT (Ad-OGT) encoding human OGT gene, adenovirus OGA (Ad-OGA) encoding human OGA gene, and adenovirus

Ser317Ala+Ser319Ala ERRγ (Ad-Ser317Ala+Ser319Ala ERRγ) were generated with the pAd-easy system as described previously [29]. All viruses were purified by using CsCl gradient protocol.

Hepatic FLAG-ERRγ complex purification and mapping of *O*-GlcNAc site using mass spectrometry

Overexpressed wild-type FLAG-ERRγ proteins from mouse liver were purified using FLAG-M2 agarose and subjected to SDS–PAGE. Purified protein was digested with trypsin (Promega, Madison, WI) (25 ng/μl) for 16 h at 37°C. After in gel digestion, tryptic peptides were separated by online reversed-phase chromatography using a Thermo Scientific Eazy nano LC II autosampler with a reversed-phase peptide trap EASY-Column (100 μm inner diameter, 2 cm length) and a reversed-phase analytical EASY-Column (75 μm inner diameter, 10 cm length, 3 μm particle size, both Thermo Scientific). Electrospray ionization was performed using a 30 μm (i.d.) nano-bore stainless steel online emitter (Thermo Scientific) and a voltage set at 2.6 V., at a flow rate of 300 nl/min. The chromatography system was coupled on-line with an LTQ Velos Orbitrap mass spectrometer. Protein identification was accomplished utilizing the Proteome Discoverer v1.3 database search engine (Thermo scientific) and searches were performed against IPI.Humanv3.87 FASTA database or ERRγ FASTA database. A fragment mass tolerance of 1.2 Da, peptide mass tolerance of 25 ppm, and maximum missed cleavage of 2 were set.

Real time quantitative RT–PCR (qPCR) analysis

Total RNA was isolated using Trizol reagent, cDNA was synthesized using a reverse transcriptase kit (Intron Biotechnology, Inc.), and qPCR was performed with SYBR green PCR kit (Enzynomics). The amount of mRNA for each gene was normalized to that of actin mRNA.

ChIP assay

Nuclear isolation of primary hepatocytes and cross-linking of protein to DNA were performed as described previously [28]. After sonication, soluble chromatin was subjected to immunoprecipitation using anti-ERRγ antibody. DNA was recovered by phenol/chloroform extraction and analyzed by PCR using primers against relevant promoters. Primer sequences: mouse PEPCK1 promoter forward: 5'- CTAGCCAGCTTTGCCTGACT-3' and reverse: 5'-GGGTCCCCACGACCTTCCA A -3'.

Western Blot Analysis

Whole cell extracts were prepared using RIPA buffer (50 mM Tris at pH 7.5, 150 mM NaCl, 1% NP-40, 5mM EDTA). Proteins from whole cell lysates were separated by 10% SDS-PAGE and then transferred to nitrocellulose membranes. The membranes were probed with different antibodies. Immunoreactive proteins were visualized using an Amersham Biosciences ECL kit (GE Healthcare) according to the manufacturer's instructions.

In Vivo Imaging

C57BL/6J mice were infected with respective viruses via tail vein injections. Four days post injection, mice were fasted for 16 h and imaged using an IVIS Lumina II imaging system (Caliper Life Sciences, Hopkinton, MA, USA) as described previously [28].

Confocal Microscopy

At 24 h after transfection, the cells were fixed with 2% formaldehyde, immunostained and subjected to observation by confocal microscopy using a laser-scanning confocal microscope (Olympus Corp., Lake Success, NY).

Pulse-chase experiment

AML12 cells were transfected with FLAG-wt ERRγ, FLAG-S317A ERRγ, FLAG-S319A ERRγ and FLAG-S317A+S319A ERRγ and incubated in methionine and cystine-free medium for 2 h. Trans-label mixture (Perkin Elmer) containing ^{35}S-methionine was added for 30 min and then cells were cultured in normal medium up to 3 h. FLAG-ERRγ was immunoprecipitated with M2 antibody in RIPA buffer and radioactive FLAG-ERRγ was detected by autoradiography.

Statistical Analyses

All values are expressed as means ± s.e.m. The significance between mean values was evaluated by two-tailed Student's *t* test.

RESULTS

ERRγ is modified by *O*-GlcNAc

ERRγ is a key positive regulator of hepatic gluconeogenesis [28]. ERRγ phosphorylation by PKB/Akt also contributes to insulin-mediated inhibition of hepatic gluconeogenesis [20]. Many factors that regulate hepatic gluconeogenesis are *O*-GlcNAcylated in various conditions [30], [7], [31]. Hence we sought to determine whether ERRγ is modified by *O*-GlcNAc. HBP intermediate GlcN treatment significantly increased ERRγ *O*-GlcNAcylation levels as well as ERRγ protein content in a dose dependent manner (Figure 1A). Consistent with a rise in ERRγ protein levels, GlcN treatment significantly reduced ERRγ ubiquitination levels and increased ERRγ transcriptional activity (Supplementary figure 1A-B). Glucose (Glc) flux through HBP regulates *O*-GlcNAcylation [1]. Therefore, to determine whether glucose could directly affect *O*-GlcNAcylation of ERRγ, mouse primary hepatocytes (MPH) were treated with 5 and 25 mM glucose. High glucose significantly increased *O*-GlcNAcylation of ERRγ along with ERRγ protein levels (Figure 1B). This was further confirmed when OGT co-transfection markedly enhanced *O*-GlcNAcylation of ERRγ (Figure 1C). Since ERRα and ERRγ are both associated with hepatic glucose metabolism, we also examined whether OGT overexpression could lead to ERRα *O*-GlcNAcylation. Unlike ERRγ, *O*-GlcNAcylation was not detected for ERRα (Figure 1D).

O-GlcNAcylation is linked with protein stability [30], [31], [32], [33]. From our results (Figure 1A-B), we speculated that *O*-GlcNAcylation could stabilize ERRγ by decreasing protein degradation. To test this, HEK 293T cells were co-transfected with ERRγ and OGA or OGT expression vectors followed by MG-132 treatment to inhibit proteasome-mediated protein

degradation. ERRγ ubiquitination levels were significantly raised and *O*-GlcNAcylation levels were decreased in presence of OGA, whereas OGT had an entirely opposite effect, suggesting that OGT triggers ERRγ *O*-GlcNAcylation that inhibits ERRγ ubiquitination and stabilizes it (Figure 1E). Next, to examine the functional implications of *O*-GlcNAcylation, reporter gene assay with transient transfection was carried out in the 293T cell line. ERRγ significantly enhanced the Sft4-luc reporter activity which was further augmented in presence of OGT. OGA had an inverse effect to that of OGT and significantly reduced ERRγ transcriptional activity. However, ERRα could not markedly activate the reporter gene even in presence of OGT (Figure 1F). Activation of the Gal4-tk-luc reporter gene by Gal4-ERRγ-LBD was significantly augmented by OGT, whereas OGA significantly repressed it, indicating that *O*-GlcNAcylation of ERRγ might occur in its LBD (Figure1G). Overall, these results suggest that ERRγ is subject to *O*-GlcNAcylation which in turn increases protein stability by decreasing ubiquitin mediated protein degradation and also enhances ERRγ transcriptional activity.

Glucagon increases *O*-GlcNAcylation of ERRγ

Hepatic ERRγ expression is increased by fasting-dependent activation of the CREB-CRTC2 pathway [28], [18]. Hence we sought to determine whether fasting-dependent increase in ERRγ expression is associated with *O*-GlcNAcylation. Fasting significantly enhanced *O*-GlcNAcylation of ERRγ compared to the fed state. This stands in contrast to ERRγ ubiquitination levels which were higher in the fed condition than the fasting condition, suggesting that *O*-GlcNAcylation mediates ERRγ stability in the fasting condition (Figure 2A). To confirm that *O*-GlcNAcylation mediates ERRγ stability in the fasting condition, we overexpressed OGA in this condition. Overexpression of OGA significantly reduced *O*-

GlcNAcylation of ERRγ and simultaneously increased ubiquitination of ERRγ, resulting in lowering of ERRγ abundance, unambiguously establishing that ERRγ stability is governed by *O*-GlcNAcylation in the fasting condition (Figure 2B). Increased protein stability is associated with decreased interaction between protein and E3 ubiquitin-ligases such as Mdm2 [32]. We observed that fasting increased OGT-ERRγ interactions in a time dependent manner, resulting in enhanced *O*-GlcNAcylation and reduced Mdm2-ERRγ interactions in mice (Figure 2C). The binding of OGT and ERRγ was reduced, but the levels of ERRγ *O*-GlcNAcylation were still intensified after 3 h of fasting (Figure 2C). To clarify this, we tested whether the interactions between ERRγ and OGT or OGA might be dynamically altered during the fasting period. The interaction between ERRγ and OGT increased in a fasting time manner, reaching a peak between 3-6 h and then declining, whereas the interaction between ERRγ and OGA decreased in a fasting time manner (Supplementary figure 1C), suggesting that in the fed state OGA interacts with ERRγ and destabilizes it, whereas in the fasting condition OGT interacts with ERRγ and stabilizes it. Interestingly, protein levels of both OGT and OGA were increased in the fasting (Supplementary figure 1C), which was supported by elevated OGT and OGA mRNA levels in fasting (Supplementary figure 1D). In spite of low circulating glucose, fasting promoted *O*-GlcNAcylation of ERRγ. Hence we speculate that glucagon could be more important than blood glucose for *O*-GlcNAcylation of ERRγ during fasting. To test this, we measured blood glucose and glucagon levels in a fasting time course experiment (Supplementary figure 1E-F). Blood glucose levels in fasting mice decreased from 0 to 12 h, whereas serum glucagon levels steadily increased from 0 h, reaching a peak at 6 h followed by a decrease at 12 h, though it remained significantly higher at 12 h than at 0 h. ERRγ *O*-GlcNAcylation levels gradually increased from 0 h, reaching a peak at 6 h and then remaining almost the same until 12 h, suggesting that

circulating glucagon levels are more important than circulating glucose levels for *O*-GlcNAcylation of ERRγ during fasting.

Glucagon increases hepatic ERRγ transcriptional activity during fasting [28]. Thus we sought to ascertain whether glucagon increases ERRγ transcriptional activity by affecting *O*-GlcNAcylation. Glucagon treatment significantly increased ERRγ *O*-GlcNAcylation levels resulting in higher protein stability through reduced ERRγ ubiquitination (Figure 2D). As both high glucose (Figure 1B) and glucagon (Figure 2D) induced *O*-GlcNAcylation, we tested which is more important for *O*-GlcNAcylation of ERRγ. Both high levels of glucose and glucagon increased ERRγ *O*-GlcNAcylation levels and total protein levels. They have a cumulative effect when applied together (Supplementary figure 1G), but unlike glucagon, glucose did not increase ERRγ mRNA levels (Supplementary figure 1H). The notion that *O*-GlcNAcylation mediates the effect of glucagon on ERRγ protein stability was further corroborated when overexpression of OGA significantly reduced both *O*-GlcNAcylation and protein levels of ERRγ (Figure 2E). Insulin induced by feeding suppresses ERRγ transcriptional activity as well as gene expression [28], [20]. Thus we speculate that insulin may inhibit *O*-GlcNAcylation of ERRγ leading to decreased protein stability. As we expected, glucagon induced ERRγ *O*-GlcNAcylation was significantly suppressed by insulin treatment in AML12 cells. ERRγ ubiquitination was markedly enhanced in presence of insulin compared to glucagon treatment resulting in lower protein stability (Figure 2F). Taken together, these results indicate that fasting increases *O*-GlcNAcylation of ERRγ leading to protein stability, whereas feeding acts reciprocally to degrade ERRγ by suppressing its *O*-GlcNAcylation.

ERRγ is modified by *O*-GlcNAc at Ser317 and Ser319

In order to identify the *O*-GlcNAc site of ERRγ we infected mouse with Ad-FLAG-ERRγ and extracted the ERRγ protein from liver tissue through immunoprecipitation (Figure 3A-B). The mass spectrometry results show that Ser317 and Ser319 of ERRγ are *O*-GlcNAcylated (Supplementary Figure 2-3). The primary structure of ERRγ revealed that Ser317 and Ser319 were present in the LBD of ERRγ (Figure 3C) which was consistent with the previous result that suggested *O*-GlcNAcylation site is in the LBD (Figure 1G). However, only Ser317 was conserved in ERRα, ERRβ and ERRγ (Figure 3C). The three dimensional structure of ERRγ-LBD provides a comprehensive view of the *O*-GlcNAcylation site. The two *O*-GcNAcylated serine residues are located at the end of helix5 of the reported ERRγ-LBD structures, which is locally stabilized with helix 6, helix 7 and a couple of strands. While Ser319 is completely exposed to the solvent accessible surface, Ser317 is partially hidden (Figure 3D). To verify the specific *O*-GlcNAcylation sites indicated by mass analysis, we constructed three site-specific point mutant cDNAs of ERRγ, Ser317Ala ERRγ, Ser319Ala ERRγ, and Ser317Ala+Ser319Ala ERRγ. The single mutants (Ser317Ala ERRγ and Ser319Ala ERRγ) showed less *O*-GlcNAcylation compared to wild-type ERRγ, whereas the double mutant (Ser317Ala+Ser319Ala) showed complete absence of an *O*-GlcNAc signal in the presence of GlcN (Figure 3E). Interestingly, even though the single mutants showed higher *O*-GlcNAcylation than the double mutant, all three mutants were highly ubiquitinated compared to wild-type in presence of GlcN, unambiguously suggesting that *O*-GlcNAcylation of both Ser317 and Ser319 is required for ERRγ protein stability (Figure 3E). Consistent with these findings, we noticed that all three mutants showed significant lower stability compared to wild-type in pulse-chase experiment, demonstrating the importance of *O*-GlcNAcylation in ERRγ protein stability

(Figure 3F). This was further confirmed when all three mutants showed significantly reduced protein levels in the presence of cycloheximide, a protein synthesis inhibitor (Supplementary figure 4A). Next, reporter gene assay reveled that unlike wild-type, the mutant ERRγ's had no significant transcriptional activity, suggesting that O-GlcNAcylation is required for ERRγ transcriptional activity as well (Figure 3G). All three mutants were unable to bind to the PEPCK promoter revealing why they had no transcriptional activity (Figure 3H). Collectively, these results illustrate that *O*-GlcNAcylation stabilizes ERRγ and increases its transcriptional activity.

_O_-GlcNAcylation affects ERRγ-PGC-1α interaction but not ERRγ cellular localization

Increase in transcriptional activity of transcription factors in response to *O*-GlcNAcylation was previously linked to their nuclear transport [7], [34]. Since the *O*-GlcNAcylation mutant ERRγ had practically no transcriptional activity compared to wild-type (Figure 3G-H), we speculate that the *O*-GlcNAcylation mutant may not translocate into the nucleus. Unexpectedly, the Ser317Ala+Ser319Ala ERRγ was located in the nucleus, indicating that sub-cellular localization of ERRγ was not governed by *O*-GlcNAcylation (Figure 4A). Transcriptional co-activator PGC-1α interacts with ERRγ and is critical for ERRγ transcriptional activity [28]. Hence, we examined whether PGC-1α could interact with Ser317Ala+Ser319Ala ERRγ. In AML12 cells, GlcN treatment significantly augmented *O*-GlcNAcylation of ERRγ as well as ERRγ-PGC-1α interaction, whereas inhibiting HBP by treating with DON, an inhibitor of GFAT, the rate-limiting enzyme of HBP, significantly reduced *O*-GlcNAcylation of ERRγ as well as ERRγ-PGC-1α interaction. We could not detect any interaction between ERRγ Ser317Ala+Ser319Ala and PGC-1α, supporting the idea that the HBP mediates ERRγ-PGC-1α interaction (Figure 4B). We also observed that GlcN treatment increased PGC-1α protein levels

(Figure 4B), but not mRNA levels (Supplementary figure 4B). The rise in PGC-1α protein levels could be due to the fact that *O*-GlcNAcylation also stabilizes PGC-1α protein [30]. Next, STZ treatment, an inhibitor of OGA and promoter of *O*-GlcNAcylation [7], [35], significantly augmented PGC-1α-ERRγ interaction, demonstrating that OGA inhibition enhances *O*-GlcNAcylation of ERRγ that results in substantial increase in PGC-1α-ERRγ interaction (Figure 4C). Along with ERRγ (FLAG), PGC-1α (HA) protein levels were also elevated in response to STZ treatment (Figure 4C), which is consistent with figure 4B where GlcN treatment elevated PGC-1α protein levels. Next, we performed *in vitro* interaction study between PGC-1α and Gal4 construct containing either wild-type or Ser317Ala+Ser319Ala ERRγ-LBD as the LBD contains the *O*-GlcNAcylation site (Figure 3C). Similar to Gal4-wild-type ERRγ-LBD, Gal4-Ser317Ala+Ser319Ala ERRγ-LBD protein was as stable as the wild-type one, but we could not detect any interaction between PGC-1α and Gal4-Ser317Ala+Ser319Ala ERRγ-LBD, suggesting that *O*-GlcNAcylation in the LBD regulates ERRγ-PGC-1α interaction (Figure 4D). Similar to the double mutant, the two single mutants also could not interact with PGC-1α (Supplementary figure 4C). Gal4-tk-Luc reporter gene assay revealed that Gal4-Ser317Ala+Ser319Ala ERRγ-LBD was incapable of activating the reporter gene in the presence of PGC-1α (Figure 4E). Moreover, Gal4-Ser317Ala+Ser319Ala ERRγ-LBD was also unable to activate the reporter gene even in presence of GlcN or OGT (Supplementary figure 4D). Taken together, these results demonstrate that *O*-GlcNAcylation regulates ERRγ-PGC-1α interaction critical to ERRγ transcriptional activity.

_O_-GlcNAcylation regulates ERRγ mediated gluconeogenic gene expression

HBP induces gluconeogenic enzymes gene expression through *O*-GlcNAcylation [7], [30]. ERRγ is a key positive regulator of gluconeogenic enzymes gene expression [28], [18]. Our previous results described that ERRγ was *O*-GlcNAcylated through HBP (Figure 1A, 4B-C). Therefore, to determine the contribution of *O*-GlcNAcylated ERRγ in HBP induced gluconeogenesis in MPH, we knocked down endogenous ERRγ. ERRγ knockdown markedly reduced GlcN induced PEPCK and G6Pase protein levels (Figure 5A). OGT overexpression leads to induction of gluconeogenesis and OGT knockdown improves glucose homeostasis in diabetic mice [7], [30]. OGT overexpression significantly increased PEPCK and G6Pase mRNA levels, and this increase in mRNA levels was greatly suppressed by ERRγ knockdown in MPH (Figure 5B, from left $1^{st}/2^{nd}$ panel). In line with PEPCK and G6Pase mRNA levels results, glucose production was also significantly reduced in response to ERRγ knock down (Figure 5B, from left 4th panel). Effectiveness of OGT overexpression was confirmed by western blot analyses (Supplementary figure 4E). Next, to examine the effect of glucose or GlcN on gluconeogenic gene promoter activity, we used wild-type and ERRE mutant PEPCK promoter which is devoid of ERRγ binding site. Exposure to glucose or GlcN increased wild-type promoter activity but this increase was greatly reduced with the ERRE mutant PEPCK promoter (Figure 5C). In a parallel approach, 293T cells were transfected with wild-type PEPCK promoter along with wild-type and Ser317Ala+Ser319Ala ERRγ. Wild-type ERRγ considerably increased the promoter activity which was further augmented in presence of OGT, whereas OGA co-expression greatly impaired ERRγ effect. While at the same time, Ser317Ala+Ser319Ala ERRγ could not greatly activate the promoter (Figure 5D). Next, ChIP assay was performed in MPH to monitor the effect of HBP inhibition on ERRγ recruitment to the endogenous PEPCK gene promoter. Under basal conditions, ERRγ occupied the PEPCK promoter. However, GlcN

treatment significantly augmented ERRγ occupancy on the PEPCK promoter, whereas HBP inhibition by DON treatment markedly diminished the occupancy. We also observed a similar binding pattern of PGC-1α (Figure 5E). Together, these results demonstrate that *O*-GlcNAcylation by HBP governs gluconeogenic activity of ERRγ.

ERRγ *O*-GlcNAcylation is required for hepatic gluconeogenesis

Diabetic conditions induce ERRγ gene expression and promote gluconeogenesis [18]. Hence, we speculated that ERRγ could be *O*-GlcNAcylated under diabetic conditions. As we expected, *O*-GlcNAcylation of ERRγ was greatly increased in HFD fed, *ob/ob* and *db/db* mice (Figure 6A-B). Previously it was reported that diabetic conditions promoted OGT gene expression [7]. We also noticed a significant increase in OGT mRNA levels in HFD-induced diabetic mouse, although, OGA mRNA levels were also elevated (Supplementary figure 4F). Overexpression of ERRγ promotes hepatic gluconeogenesis and elevates blood sugar levels [28], [18]. Therefore we compared the effect of wild-type and Ser317Ala+Ser319Ala ERRγ overexpression in mouse liver. In accordance with previous results, glucose excursion during intraperitoneal glucose tolerance test (IPGTT) was significantly higher in Ad-wild-type ERRγ–injected mice compared to control mice, but Ad-Ser317Ala+Ser319Ala ERRγ-injected mice showed normal blood glucose levels (Figure 6C). Fasting blood glucose levels and PEPCK and G6Pase mRNA levels were significantly higher for Ad-wild-type ERRγ-infection compared to Ad-Ser317Ala+Ser319Ala ERRγ (Figure 6D). Effectiveness of ERRγ overexpression was confirmed by western blot analyses (Supplementary figure 4G). Next, to negate the effect of *O*-GlcNAcylation we overexpressed OGA in mouse liver. Disrupting *O*-GlcNAcylation of ERRγ in mice infected with Ad-wild-type ERRγ through overexpression of hepatic OGA by Ad-OGA

greatly lowered the gluconeogenic profile (Figure 6E). Effectiveness of ERRγ overexpression was confirmed by western blot analyses (Supplementary figure 4H). Finally, on the basis of the previous result (Figure 6C-D), we performed *in vivo* imaging analysis to verify the effect of *O*-GlcNAcylation of ERRγ on hepatic gluconeogenesis at the transcriptional levels. Ad-wild-type ERRγ-dependent induction of PEPCK promoter activity was significantly reduced in mice injected with Ad-Ser317Ala+Ser319Ala ERRγ (Figure 6F). Overall, these results suggest that *O*-GlcNAcylation is prerequisite for ERRγ to trigger hepatic gluconeogenesis.

DISCUSSION

Several transcription factors promote gluconeogenesis in the fasted state and type 2 diabetes. We hypothesize that in the fasting and diabetic states gluconeogenesis generates fructose-6-phosphate, which is utilized by HBP to *O*-GlcNAcylate transcription factors and co-activators to further promote gluconeogenesis. In the current study, we show that ERRγ is stabilized by *O*-GlcNAcylation in the fasted and diabetic states to promote gluconeogenic gene induction. Hence, we suggest a positive feed-forward loop in which glucose entry into the HBP promotes gluconeogenesis in the fasting and diabetic conditions in the liver.

Glucagon-insulin crosstalk regulates ERRγ protein stability and transcriptional activity [28], [20]. Herein, we investigated whether ERRγ protein stability and transcriptional activity is influenced by *O*-GlcNAcylation. In fact, glucagon stabilized ERRγ by promoting its *O*-GlcNAcylation (Figure 2D-F). *O*-GlcNAcylation can increase protein stability and transcriptional activity by inhibiting ubiquitination or promoting deubiquitination [30], [31], [33]. It can also reduce protein stability and transcriptional activity by increasing ubiquitination [36], [37]. However, we observed that *O*-GlcNAcylation stabilized ERRγ protein by inhibiting its ubiquitination (Figure 2D-F). Our results clearly demonstrated that incremental *O*-GlcNAcylation mediated reduction in ubiquitination was a result of greater inhibition of the interaction between ERRγ and E3 ubiquitin ligase Mdm2 that resulted in increased protein stability (Figure 2C). Phosphorylation of GFAT1 by cAMP-dependent protein kinase blocks its enzyme activity [38], whereas phosphorylation of GFAT2 by cAMP-dependent protein kinase increases its enzyme activity [39]. Our observation that glucagon robustly enhances *O*-GlcNAcylation of ERRγ and insulin inhibits it (Figure 2F) could be due to GFAT2 activation. *O*-

GlcNAcylation can affect transcription factors by modifying key residues involved in their interaction with co-activators [40]. It can also induce important conformational changes within transcription factors, which might have a direct impact on their activity, as demonstrated for the estrogen receptor [41]. Three dimensional structural features of ERRγ also suggest that *O*-GlcNAcylation may trigger a conformational change of ERRγ-LBD that contains the AF-2 domain (Figure 3D). This probable conformational change may be crucial for inhibition of ubiquitination and ERRγ-PGC-1α interaction. Perhaps, S317A ERRγ and S319A ERRγ, in spite of being partially *O*-GlcNAcylated, were heavily ubiquitinated (Figure 3E) and were unable to interact with PGC-1α (Supplementary figure 4C). The two single mutants may not attain the desired conformational change required to inhibit ubiquitination and interact with co-activator PGC-1α due to incomplete *O*-GlcNAcylation. Further investigation is required to confirm whether *O*-GlcNAcylation influences ERRγ-LBD structure. Previously Yang et al. reported that the transcripts of ERRγ followed a cyclic pattern in its diurnal rhythmicity in the liver [42]. ERRγ transcripts reach maximum levels in the liver during the day time. The observed result of O-GlcNAcylation mediated stability of ERRγ may have been influenced by the diurnal rhythmicity in the liver.

O-GlcNAcylation takes place in response to high glucose or insulin [43], [31], [44]. PGC-1α and CRTC2 undergo O-GlcNAcylation in hyperglycemic and hyperinsulinemic diabetic mouse [30], [7]. Interestingly, low glucose conditions also promote O-GlcNAcylation [30], [7], [9]. Glucose deprivation induces protein *O*-GlcNAcylation and OGT expression as well [45]. All these reports suggest that both high and low glucose conditions promote O-GlcNAcylation *in vitro* and *in vivo*. Glucose in the form of fructose-6-phosphate is utilized by hexosamine

biosynthetic pathway to *O*-GlcNAcylate proteins under different conditions. In the fed conditions, high circulating glucose could be converted to fructose-6-phosphate and utilized in O-GlcNAcylation. Although the circulating glucose concentration is high in the diabetic condition, the diabetic condition differs from the fed condition in that the activity of glucokinase, which converts glucose to glucose-6-phosphate, is low in the liver [46], [47], [48]. Therefore, circulating glucose is less readily converted to fructose-6-phosphate in the diabetic condition. In the diabetic conditions hepatic gluconeogenesis is significantly upregulated [49], producing fructose-6-phosphate, which could be utilized in O-GlcNAcylation. Furthermore, in low circulating glucose (fasting) conditions, glycogenolysis and gluconeogenesis are both called into play to maintain blood glucose levels. During early fasting glycogenolysis, stimulated by glucagon, produces glucose-6-phosphate which is in equilibrium with fructose-6-phosphate [50]. Therefore, glycogenolysis, especially during early fasting, is surely a major source of fructose-6-phosphate. During short-term fasting, glucagon also triggers the initial induction of hepatic gluconeogenesis through activation of CREB-CRTC2 [7]. In prolonged fasting, PGC-1α, FOXO1 and ERRγ promote hepatic gluconeogenesis [30], [51], [28]. During that initial induction period (short-term fasting), hepatic glycogenolysis and gluconeogenesis produce fructose-6-phosphate which might be utilized to *O*-GlcNAcylate ERRγ to further promote gluconeogenesis during prolonged fasting. We observed that blood glucose levels were decreased during fasting in a time dependent manner, whereas serum glucagon levels and ERRγ *O*-GlcNAcylation levels were steadily increased (Supplementary figure 1E-F), indicating that circulating glucagon levels are more important than circulating glucose levels for *O*-GlcNAcylation of ERRγ in fasting. Moreover, OGT mRNA levels were significantly enhanced in response to fasting, even though OGA mRNA levels were also enhanced but it was less

significant compared to OGT (Supplementary figure 1D). Enhanced OGT mRNA levels could also be responsible for fasting dependent O-GlcNAcylation of ERRγ.

Conserved ERRγ response element (ERRE) on the PEPCK promoter is required for the transcription of that gene in response to fasting and diabetes mediated gluconeogenesis [28], [18], hence we explored the role of ERRγ in HBP mediated gluconeogenesis. Loss of endogenous ERRγ in primary hepatocytes led to a significant decrease in HBP-induced gluconeogenic profile (Figure 5), implying the importance of *O*-GlcNAcylation of ERRγ in the context of gluconeogenesis. Diabetic conditions promote *O*-GlcNAcylation mediated gluconeogenesis in the diabetic mice [7], [30]. As a matter of fact, ERRγ was highly *O*-GlcNAcylated in diabetic mice (Figure 6A-B). Hepatic overexpression of wild-type ERRγ caused glucose intolerance with hyperglycaemia, whereas *O*-GlcNAcylation mutant ERRγ overexpression showed glucose tolerance with euglycaemia in mice (Figure 6C-D). *O*-GlcNAcylation was blocked by using either OGT or GFAT inhibitor or by enzymatically modulating OGA or OGT expression to investigate the effect of their inhibition on glycemia in diabetic mice. The OGT inhibitor alloxan was used in many studies [52], [53], [54], but it has wide off-target effects and general cellular toxicity [55]. Another OGT inhibitor Ac_4-5S-GlcNAc was used in wide range of studies [56], [57], [58], but it affects other glycosyltransferase and impairs N-glycosylation and extracellular glycan synthesis in cultured cell lines [59]. Moreover, the enzymatic approach modulating OGA or OGT expression was successfully utilized to restore glucose homeostasis. Overexpression of hepatic OGA or knockdown of hepatic OGT inhibited aberrant gluconeogenesis and significantly improved glycemic conditions in diabetic mice [7], [30], [31]. We observed that disruption of *O*-

GlcNAcylation by hepatic OGA overexpression reduced gluconeogenic profile in normal mice expressing Ad-ERRγ (Figure 6E), unambiguously illustrating that *O*-GlcNAcylation is prerequisite for gluconeogenic function of ERRγ.

We conclude that the fasting and diabetic conditions promote *O*-GlcNAcylation of ERRγ. *O*-GlcNAcylation is imperative for ERRγ protein stability, and enhances gluconeogenic activity of ERRγ. The fed state, however, reduces *O*-GlcNAcylation of ERRγ, resulting in ubiquitin-mediated degradation of ERRγ (Figure 6G). Our results indicate a vital role for *O*-GlcNAcylation of ERRγ in maintaining normal glucose levels during fasting and also in mediating the elevated blood glucose levels in type 2 diabetes. Hence, pharmacological inhibition of *O*-GlcNAcylation mediated hyper-activation of ERRγ might provide a pathway for preventing hyperglycaemia and treating type2 diabetes.

ACKNOWLEDGEMENTS

We would like to thank David Moore (Baylor College of Medicine, Houston, TX, USA) and Seok-Yong Choi (Department of Biomedical Sciences, Chonnam National University Medical School, Gwangju, Republic of Korea) for helpful discussion and Ji Min Lee, Yong Soo Lee, Ki Sun Kim, Soon-Young Na, Yaochen Zhang for technical assistance. This work was supported by National Creative Research Initiatives Grant (20110018305) through the National Research Foundation of Korea (NRF) funded by the Korean government (Ministry of Science, ICT & Future Planning) to HSC. This research was supported by the NRF funded by the Ministry of Education, Science and Technology (NRF-2013R1A2A1A01008067 and NRF-2015M3A9B6073840) to JWC.

The authors declare that they have no conflict of interest.

JM and HSC conceived and designed research; JM performed experiments; YHK performed mouse *in vivo* imaging; HBK, BGK and SHK performed LC-MS/MS CID site mapping analysis for identification of *O*-GlcNAcylation sites; JM, HSC, JSK, JWC, IKL, SHK, CHL, RAH analyzed the data; DKK, YSJ, EKY, JWC provided reagents/materials/ analysis tools; JM, HSC Wrote the paper. Professor Hueng-Sik Choi is the guarantor of this work and, as such, had full access to all the data in the study and takes responsibility for the integrity of the data and for the accuracy of the data analysis.

REFERENCES

1. Hart, G.W., et al., Cross talk between O-GlcNAcylation and phosphorylation: roles in signaling, transcription, and chronic disease. Annu Rev Biochem., 2011. **80**: p. 825-58.
2. Hebert, L.F., Jr., et al., Overexpression of glutamine:fructose-6-phosphate amidotransferase in transgenic mice leads to insulin resistance. J Clin Invest, 1996. **98**(4): p. 930-6.
3. Veerababu, G., et al., Overexpression of glutamine: fructose-6-phosphate amidotransferase in the liver of transgenic mice results in enhanced glycogen storage, hyperlipidemia, obesity, and impaired glucose tolerance. Diabetes, 2000. **49**(12): p. 2070-8.
4. McClain, D.A., et al., Altered glycan-dependent signaling induces insulin resistance and hyperleptinemia. Proc Natl Acad Sci U S A, 2002. **99**(16): p. 10695-9.
5. Whelan, S.A., et al., Regulation of insulin receptor substrate 1 (IRS-1)/AKT kinase-mediated insulin signaling by O-Linked beta-N-acetylglucosamine in 3T3-L1 adipocytes. J Biol Chem. , 2010. **285**(8): p. 5204-11.
6. Yang, X., et al., Phosphoinositide signalling links O-GlcNAc transferase to insulin resistance. Nature, 2008. **451**(7181): p. 964-9.
7. Dentin, R., et al., Hepatic glucose sensing via the CREB coactivator CRTC2. Science, 2008. **319**(5868): p. 1402-5.
8. Housley, M.P., et al., O-GlcNAc regulates FoxO activation in response to glucose. J Biol Chem, 2008. **283**(24): p. 16283-92.
9. Housley, M.P., et al., A PGC-1alpha-O-GlcNAc transferase complex regulates FoxO transcription factor activity in response to glucose. J Biol Chem, 2009. **284**(8): p. 5148-57.
10. Kuo, M., et al., O-GlcNAc modification of FoxO1 increases its transcriptional activity: a role in the glucotoxicity phenomenon? Biochimie, 2008. **90**(5): p. 679-85.
11. Andrali, S.S., Q. Qian, and S. Ozcan, Glucose mediates the translocation of NeuroD1 by O-linked glycosylation. J Biol Chem, 2007. **282**(21): p. 15589-96.
12. Gao, Y., J. Miyazaki, and G.W. Hart, The transcription factor PDX-1 is post-translationally modified by O-linked N-acetylglucosamine and this modification is correlated with its DNA binding activity and insulin secretion in min6 beta-cells. Arch Biochem Biophys. , 2003. **415**(2): p. 155-63.
13. Hong, H., L. Yang, and M.R. Stallcup, Hormone-independent transcriptional activation and coactivator binding by novel orphan nuclear receptor ERR3. J Biol Chem, 1999. **274**(32): p. 22618-26.
14. Lui, K., et al., Molecular cloning and functional study of rat estrogen receptor-related receptor gamma in rat prostatic cells. Prostate, 2006. **66**(15): p. 1600-19.
15. Zhang, Z. and C.T. Teng, Interplay between estrogen-related receptor alpha (ERRalpha) and gamma (ERRgamma) on the regulation of ERRalpha gene expression. Mol Cell Endocrinol., 2007. **264**(1-2): p. 128-41.
16. Kim, D.K., et al., Estrogen-related receptor gamma controls hepatic CB1 receptor-mediated CYP2E1 expression and oxidative liver injury by alcohol. Gut, 2013. **62**(7): p. 1044-54.

17. Kim, D.K., et al., Inverse agonist of estrogen-related receptor gamma controls Salmonella typhimurium infection by modulating host iron homeostasis. Nat Med, 2014. **20**(4): p. 419-24.
18. Kim, D.K., et al., Inverse Agonist of Nuclear Receptor ERRg Mediates Antidiabetic Effect Through Inhibition of Hepatic Gluconeogenesis. Diabetes., 2013. **62**(9): p. 3093-102.
19. Kim, D.K., et al., Estrogen-related receptor γ (ERRγ) is a novel transcriptional regulator of phosphatidic acid phosphatase, LIPIN1, and inhibits hepatic insulin signaling. J Biol Chem. , 2011. **286**(44): p. 38035-42.
20. Kim, D.K., et al., PKB/Akt phosphorylation of ERRgamma contributes to insulin-mediated inhibition of hepatic gluconeogenesis. Diabetologia, 2014. **57**(12): p. 2576-85.
21. Yoon, J.C., et al., Control of hepatic gluconeogenesis through the transcriptional coactivator PGC-1. Nature, 2001. **413**(6852): p. 131-138.
22. Puigserver, P., et al., Insulin-regulated hepatic gluconeogenesis through FOXO1-PGC-1alpha interaction. Nature. , 2003. **423**(6939): p. 550-5.
23. Koo, S.H., et al., PGC-1 promotes insulin resistance in liver through PPAR-α-dependent induction of TRB-3. Nat Med. , 2004. **10**(5): p. 530-4.
24. Kim, Y.D., et al., Metformin inhibits hepatic gluconeogenesis through AMP-activated protein kinase-dependent regulation of the orphan nuclear receptor SHP. J Biol Chem., 2012. **287**(26): p. 21628-39.
25. Xie, Y.B., et al., Transcriptional corepressor SMILE recruits SIRT1 to inhibit nuclear receptor estrogen receptor-related receptor gamma transactivation. J Biol Chem, 2009. **284**(42): p. 28762-74.
26. Sanyal, S., et al., Differential regulation of the orphan nuclear receptor small heterodimer partner (SHP) gene promoter by orphan nuclear receptor ERR isoforms. J Biol Chem, 2002. **277**(3): p. 1739-48.
27. Heard, D.J., et al., Human ERRgamma, a third member of the estrogen receptor-related receptor (ERR) subfamily of orphan nuclear receptors: tissue-specific isoforms are expressed during development and in the adult. Mol Endocrinol, 2000. **14**(3): p. 382-92.
28. Kim, D.K., et al., Orphan Nuclear Receptor Estrogen-Related Receptor γ (ERRγ) Is Key Regulator of Hepatic Gluconeogenesis. J Biol Chem, 2012. **287**(26): p. 21628-39.
29. Park, Y.Y., et al., An autoregulatory loop controlling orphan nuclear receptor DAX-1 gene expression by orphan nuclear receptor ERRgamma. Nucleic Acids Res, 2005. **33**(21): p. 6756-68.
30. Ruan, H.B., et al., O-GlcNAc transferase/host cell factor C1 complex regulates gluconeogenesis by modulating PGC-1alpha stability. Cell Metab, 2012. **16**(2): p. 226-37.
31. Guinez, C., et al., O-GlcNAcylation increases ChREBP protein content and transcriptional activity in the liver. Diabetes, 2011. **60**(5): p. 1399-413.
32. Yang, W.H., et al., Modification of p53 with O-linked N-acetylglucosamine regulates p53 activity and stability. Nat Cell Biol, 2006. **8**(10): p. 1074-83.
33. Park, S.Y., et al., Snail1 is stabilized by O-GlcNAc modification in hyperglycaemic condition. Embo Journal, 2010. **29**(22): p. 3787-3796.
34. Guinez, C., et al., O-GlcNAc glycosylation: a signal for the nuclear transport of cytosolic proteins? Int J Biochem Cell Biol, 2005. **37**(4): p. 765-74.

35. Konrad, R.J., K.M. Janowski, and J.E. Kudlow, Glucose and streptozotocin stimulate p135 O-glycosylation in pancreatic islets. Biochem Biophys Res Commun, 2000. **267**(1): p. 26-32.
36. Ji, S., et al., O-GlcNAc modification of PPARc reduces its transcriptional activity. Biochemical and Biophysical Research Communications, 2012. **417**(4): p. 1158–1163.
37. Guinez, C., et al., Protein ubiquitination is modulated by O-GlcNAc glycosylation. Faseb Journal, 2008. **22**(8): p. 2901-2911.
38. Chang, Q., et al., Phosphorylation of human glutamine : fructose-6-phosphate amidotransferase by cAMP-dependent protein kinase at serine 205 blocks the enzyme activity. Journal of Biological Chemistry, 2000. **275**(29): p. 21981-21987.
39. Hu, Y., et al., Phosphorylation of mouse glutamine-fructose-6-phosphate amidotransferase 2 (GFAT2) by cAMP-dependent protein kinase increases the enzyme activity. J Biol Chem, 2004. **279**(29): p. 29988-93.
40. Gewinner, C., et al., The coactivator of transcription CREB-binding protein interacts preferentially with the glycosylated form of Stat5. J Biol Chem, 2004. **279**(5): p. 3563-72.
41. Hart, G.W. and K. Sakabe, Fine-tuning ER-beta structure with PTMs. Chem Biol, 2006. **13**(9): p. 923-4.
42. Yang, X., et al., Nuclear receptor expression links the circadian clock to metabolism. Cell, 2006. **126**(4): p. 801-10.
43. Walgren, J.L., et al., High glucose and insulin promote O-GlcNAc modification of proteins, including alpha-tubulin. Am J Physiol Endocrinol Metab, 2003. **284**(2): p. E424-34.
44. Hanover, J.A., M.W. Krause, and D.C. Love, The hexosamine signaling pathway: O-GlcNAc cycling in feast or famine. Biochim Biophys Acta, 2010. **1800**(2): p. 80-95.
45. Cheung, W.D. and G.W. Hart, AMP-activated protein kinase and p38 MAPK activate O-GlcNAcylation of neuronal proteins during glucose deprivation. J Biol Chem, 2008. **283**(19): p. 13009-20.
46. Caro, J.F., et al., Liver glucokinase: decreased activity in patients with type II diabetes. Horm Metab Res, 1995. **27**(1): p. 19-22.
47. Torres, T.P., et al., Restoration of hepatic glucokinase expression corrects hepatic glucose flux and normalizes plasma glucose in zucker diabetic fatty rats. Diabetes, 2009. **58**(1): p. 78-86.
48. Osbak, K.K., et al., Update on Mutations in Glucokinase (GCK), Which Cause Maturity-Onset Diabetes of the Young, Permanent Neonatal Diabetes, and Hyperinsulinemic Hypoglycemia. Human Mutation, 2009. **30**(11): p. 1512-1526.
49. Consoli, A., Role of liver in pathophysiology of NIDDM. Diabetes Care, 1992. **15**(3): p. 430-41.
50. Agius, L., Targeting hepatic glucokinase in type 2 diabetes: weighing the benefits and risks. Diabetes, 2009. **58**(1): p. 18-20.
51. Zhang, K., R. Yin, and X. Yang, O-GlcNAc: A Bittersweet Switch in Liver. Front Endocrinol (Lausanne), 2014. **5**: p. 221.
52. Konrad, R.J., et al., Alloxan is an inhibitor of the enzyme O-linked N-acetylglucosamine transferase. Biochemical and Biophysical Research Communications, 2002. **293**(1): p. 207-212.

53. Liu, J., et al., Cardiovascular effects of endomorphins in alloxan-induced diabetic rats. Peptides, 2005. **26**(4): p. 607-14.
54. Xu, C., et al., O-GlcNAcylation under hypoxic conditions and its effects on the blood-retinal barrier in diabetic retinopathy. Int J Mol Med, 2014. **33**(3): p. 624-32.
55. Zhang, H., G. Gao, and U.T. Brunk, Extracellular reduction of alloxan results in oxygen radical-mediated attack on plasma and lysosomal membranes. APMIS, 1992. **100**(4): p. 317-25.
56. Donovan, K., et al., O-GlcNAc modification of transcription factor Sp1 mediates hyperglycemia-induced VEGF-A upregulation in retinal cells. Invest Ophthalmol Vis Sci, 2014. **55**(12): p. 7862-73.
57. Perez-Cervera, Y., et al., Insulin signaling controls the expression of O-GlcNAc transferase and its interaction with lipid microdomains. FASEB J, 2013. **27**(9): p. 3478-86.
58. Ma, Z., D.J. Vocadlo, and K. Vosseller, Hyper-O-GlcNAcylation is anti-apoptotic and maintains constitutive NF-κB activity in pancreatic cancer cells. J Biol Chem., 2013. **288**(21): p. 15121-30.
59. Ortiz-Meoz, R.F., et al., A Small Molecule That Inhibits OGT Activity in Cells. Acs Chemical Biology, 2015. **10**(6): p. 1392-1397.

FIGURE LEGENDS

Figure 1. ERRγ is modified by *O*-GlcNAcylation. (A) Mouse primary hepatocytes were treated with GlcN in a dose dependent manner for 6 h and subsequently immunoprecipitated with ERRγ antibody. Total proteins were analyzed for the *O*-GlcNAcylation by immunoblot with *O*-GlcNAc, OGT, ERRγ and α-tubulin antibodies. (B) Mouse primary hepatocytes were incubated in 5 mM or 25 mM glucose media overnight followed by immunoprecipitation with ERRγ antibody and immunoblot with *O*-GlcNAc, ERRγ and α-tubulin antibodies. (C, D) HEK 293T cells were transfected with expression vector for HA-ERRγ (C) and HA-ERRα (D) alone or with expression vector for FLAG-OGT, followed by immunoprecipitation with HA antibody and immunoblot with *O*-GlcNAc, HA and α-tubulin antibodies. (E) HEK 293T cells transfected with plasmids encoding HA-ERRγ and FLAG-OGA or FLAG-OGT. At 24 h after transfection cells were treated with MG-132 (10μM) for 6 h followed by immunoprecipitation with HA antibody and immunoblot with *O*-GlcNAc, ubiquitin (Ub), HA and α-tubulin antibodies. (F) HEK 293T cells were transfected with Sft4-luc along with the indicated plasmids. (G) HEK 293T cells were transfected with Gal4-tk-luc along with the indicated plasmids. *$p < 0.05$, and **$P < 0.005$ using Student's t-test. Error bars show ± s.e.m.

Figure 2. Glucagon increases *O*-GlcNAcylation of ERRγ. (A) C57BL/6 mice (n=5) were fasted for 6 h and refed for 2 h, followed by liver tissue isolation. Immunoprecipitation with ERRγ antibody and immunoblot with *O*-GlcNAc, Ub, ERRγ and α-tubulin antibodies were performed. All of the samples were combined for western blot analyses. (B) Ad-green fluorescent protein (GFP) or Ad-OGA was administered via tail-vein injection into C57BL/6 mice (n=6). At day 6 after injection, mice were fasted for 6 h and sacrificed. Liver tissue from

mice was homogenized for immunoprecipitation with ERRγ antibody and immunoblot with *O*-GlcNAc, Ub, ERRγ and α-tubulin antibodies. All of the samples were combined for western blot analyses. (C) Liver tissue from C57BL/6 mice (n=5) fasted for different time points as indicated, was homogenized for immunoprecipitation with ERRγ antibody and immunoblot with *O*-GlcNAc, OGT, Mdm2, ERRγ and α-tubulin antibodies. All of the samples were combined for western blot analyses. (D) AML12 cells were transfected with FLAG-ERRγ. At 24 h post transfection, cells were incubated with vehicle or glucagon (100 nM) for different time points as indicated. Immunoprecipitation with FLAG antibody and immunoblot with *O*-GlcNAc, Ub, FLAG and α-tubulin antibodies were performed. (E) AML12 cells were transfected with FLAG-ERRγ. At 24 h post transfection, cells were infected with Ad-GFP or Ad-OGA as indicated. At 24 h post infection, cells were incubated with glucagon (100 nM) for 6 h followed by immunoprecipitation with FLAG antibody and immunoblot with *O*-GlcNAc, Ub, FLAG and α-tubulin antibodies were performed. (F) AML12 cells were transfected with FLAG-ERRγ. At 24 h post transfection, cells were incubated with glucagon (100 nM) for 6 h or glucagon (100 nM) for 6 h followed by insulin (100 nM) for 6 h. Immunoprecipitation with FLAG antibody and immunoblot with *O*-GlcNAc, OGT, Ub, FLAG and α-tubulin antibodies were performed.

Figure 3. ERRγ is modified by *O*-GlcNAcylation at Ser317 and Ser319. (A) C57BL/6 mice (n=5) were injected via tail veins with adenoviral vector expressing FLAG-ERRγ. Six days later, mice were fasted for 6 h and liver extracts were prepared. The FLAG-ERRγ was purified using Anti-FLAG M2 agarose. (B) Proteins were separated using SDS-PAGE and stained by colloidal Coomassie blue. (C) Schematic diagram of ERRγ structure (amino acids, 1–458). ERRγ consists of N-terminal domain, DNA-binding domain (DBD), hinge domain, Ligand-binding

domain (LBD) and C-terminal domain. ERRγ is *O*-GlcNAcylated at S317 and S319. The amino acid sequences of ERR family members, ERRα, ERRβ, and ERRγ are given below. (D) Two serine residues of ERRγ-LBD. Twelve LBD structures (PDB IDs 2ewp, 2gpp, 2gp7, and 2p7z) were superimposed, which showed root-mean-square deviation values of less than 0.4 Å for all the aligned residues. ERRγ-AF-2 domain is represented as an orange color surface; ERRγ-LBD as a grey-colored surface with two serine residues in space-filling models in the left and below-right panels. On the upper-right panel, the superimposed ERRγ-LBD structures are displayed with ribbons and differentiated by colors; two serine residues are drawn as stick models. (E) AML12 cells were transfected with plasmids encoding FLAG-wt ERRγ, FLAG-Ser317Ala ERRγ, FLAG-Ser319Ala ERRγ and FLAG-Ser317Ala+Ser319Ala ERRγ. At 24 h after transfection cells were treated with GlcN (10 mM) for 6 h and MG-132 (10 μM) for 6 h followed by immunoprecipitation with FLAG antibody and immunoblot with *O*-GlcNAc, Ub, FLAG and α-tubulin antibodies. (F) AML12 cells transfected with FLAG-wt ERRγ, FLAG-S317A ERRγ, FLAG-S319A ERRγ and FLAG-S317A+S319A ERRγ were metabolically labeled for 30 min followed by chase for the indicated times. FLAG-ERRγ was immunoprecipitated with M2 antibody and detected by autoradiography. (G) ERRγ-dependent activation of the Sft4-luc. Transient transfection was performed in HEK 293T cells with the indicated plasmid DNAs. (H) ChIP assay showing the occupancy of wild-type ERRγ, S317A ERRγ, S319A ERRγ and S317A+S319A ERRγ on ERRE1 of PEPCK1 promoter from DMSO and GlcN-treated AML12 cells. ***P <0.0005 using Student's t-test. Error bars show ± s.e.m.

Figure 4. *O*-GlcNAcylation affects ERRγ-PGC-1α interaction but not ERRγ cellular localization. (A) Immunocytochemistry showing subcellular localization of wild-type and

mutant ERRγ in AML12. The cells were transfected with plasmids expressing FLAG-wt ERRγ and FLAG-Ser317Ala+Ser319Ala ERRγ. At 24 h after transfection cells were fixed, immunostained and observed by confocal microscopy. (B) AML12 cells were transfected with plasmids encoding FLAG-wt ERRγ and FLAG-Ser317Ala+Ser319Ala ERRγ. At 24 h after transfection cells were treated with MG-132 (10 μM) and DMSO or GlcN (10 mM) or DON (40 μM) for 6 h followed by immunoprecipitation with FLAG antibody and immunoblot with *O*-GlcNAc, PGC-1α, FLAG, and α-tubulin antibodies. (C) AML12 cells were transfected with plasmids encoding FLAG-wt ERRγ and HA-PGC-1α. At 24 h after transfection cells were treated with DMSO or OGA inhibitor STZ (5 mM) for 6 h followed by immunoprecipitation with HA antibody and immunoblot with FLAG, HA and α-tubulin antibodies. (D) HEK 293T cells were transfected with plasmids encoding Gal4-wt ERRγ-LBD, Gal4-Ser317Ala+Ser319Ala ERRγ-LBD and HA-PGC-1α. At 24 h post transfection immunoprecipitation with HA antibody and immunoblot with Gal4 and HA antibodies were performed. (E) HEK 293T cells were transfected with Gal4-tk-luc along with the indicated plasmids. *$p < 0.05$ using Student's t-test. Error bars show ± s.e.m.

Figure 5. *O*-GlcNAcylation regulates ERRγ transcriptional activity. (A) Effect of ERRγ knockdown on GlcN-induced gluconeogenic genes in mouse primary hepatocytes. Hepatocytes were infected with Ad-US or Ad-shERRγ. At 48 h post infection, cells were treated with DMSO or GlcN (10 mM) for 6 h followed by immunoblot with PEPCK, G6Pase, ERRγ and α-tubulin antibodies. (B) Effect of ERRγ knockdown on basal and OGT-induced gluconeogenic genes in mouse primary hepatocytes. Glucose output assay was performed in mouse primary hepatocytes. (C) Effect of Glc and GlcN on wild-type (wt) and ERRγ binding site (ERRE)

mutant PEPCK-luc. HEK 293T cells were transfected with indicated plasmids followed by Glc or GlcN treatment. (D) *O*-GlcNAcylation-dependent activation of the PEPCK1-luc by ERRγ. HEK 293T cells were transfected with indicated plasmids. (E) ChIP assay showing the occupancy of ERRγ on ERRE1 of PEPCK1 promoter from GlcN, DON-treated mouse primary hepatocytes. *p <0.05, and **P <0.005 using Student's t-test. Error bars show ± s.e.m.

Figure 6. ERRγ *O*-GlcNAcylation required for hepatic gluconeogenesis. (A-B) *O*-GlcNAcylation of ERRγ in diabetic conditions, ERRγ was immunoprecipitated with ERRγ antibody followed by immunoblot with *O*-GlcNAc, ERRγ, PEPCK and α-tubulin antibodies from liver tissue of C57BL/6 mice (n=3) fed with normal chow diet (NCD) and high fat diet (HFD) (A), from wild-type, *ob/ob* and *db/db* mice (n=3) (B). (C) Ad-GFP, Ad-wt ERRγ or Ad-Ser317Ala+Ser319Ala ERRγ were administered via tail-vein injection into C57BL/6 mice (n=5). Glucose tolerance test at day 5 after injection. Glucose was measured at the indicated times after 1 g/kg intraperitoneal glucose injection. (D) (Left panel) 4 h fasting blood glucose levels in C57BL/6 mice (n=5) at day 6 after Ad-GFP, Ad-wt ERRγ or Ad-Ser317Ala+Ser319Ala ERRγ injection. (Middle and right panel) qPCR analyses of total RNA isolated from liver at day 7 after injection. (E) (Left panel) 4 h fasting blood glucose levels in C57BL/6 mice (n=5) at day 6 after Ad-GFP, Ad-ERRγ or Ad-ERRγ + Ad-OGA injection. (Middle and right panel) qPCR analyses of total RNA isolated from mice liver at day 7 after injection. (F) (Left) *In vivo* imaging of hepatic PEPCK1-luciferase (Ad-PEPCK1-luc) activity in presence of Ad-GFP or Ad-wt ERRγ or Ad-Ser317Ala+Ser319Ala ERRγ in fasted (16 h) C57BL/6 mice (n=3). (Right) Quantitation of luciferase activity is also shown. (G) Schematic representation of the proposed model that the fasting and diabetic conditions promote *O*-GlcNAcylation of ERRγ. *O*-GlcNAcylation is

imperative for ERRγ protein stability, and enhances gluconeogenic activity of ERRγ. Fed state, however, reduces *O*-GlcNAcylation of ERRγ, resulting in ubiquitin-mediated degradation of ERRγ. *p <0.05, **P <0.005, and ***P <0.0005 using Student's t-test. Error bars show ± s.e.m.

Figure 1

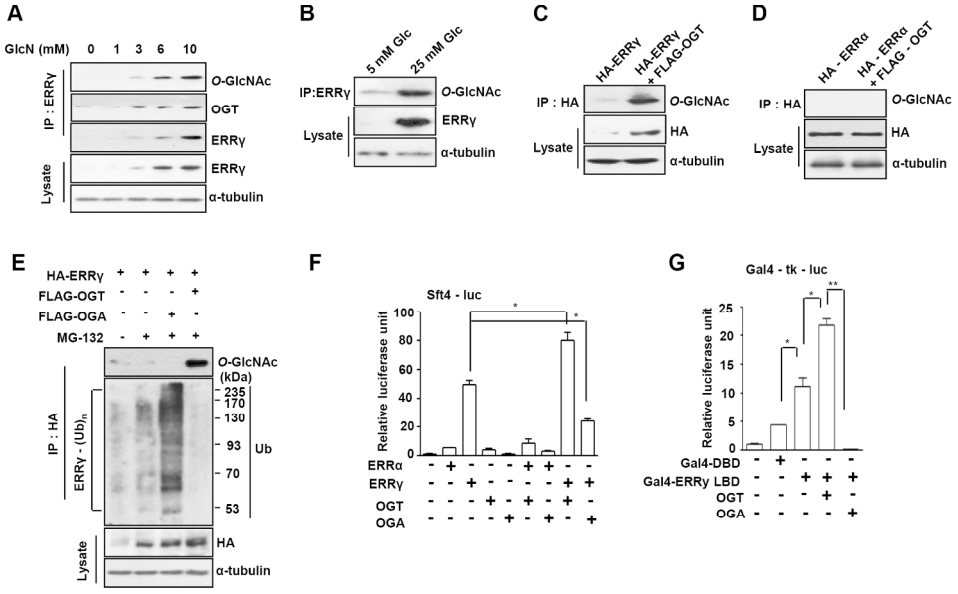

Figure 1
190x136mm (300 x 300 DPI)

Figure 2

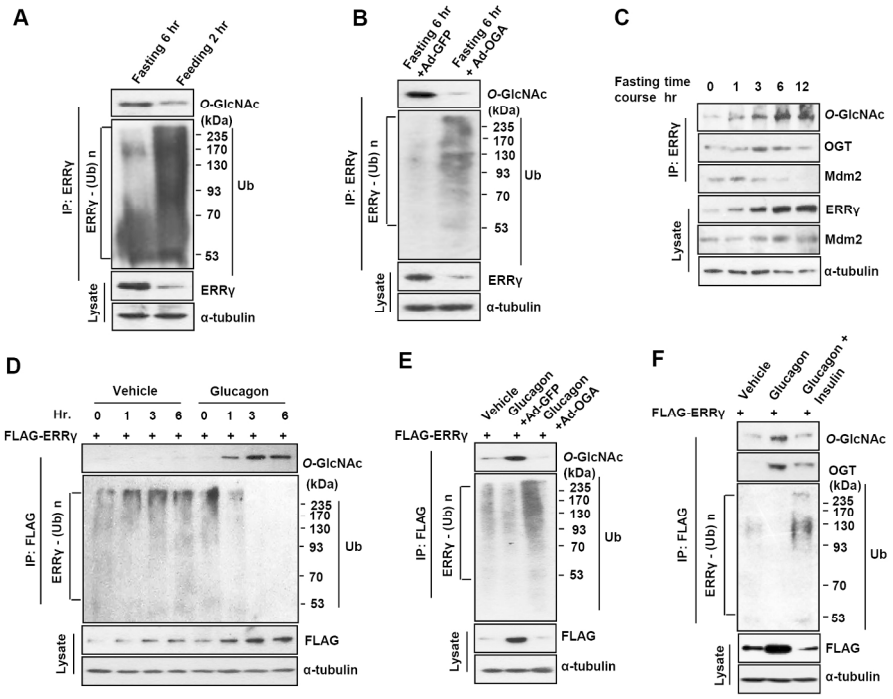

Figure 2
190x155mm (300 x 300 DPI)

Figure 3

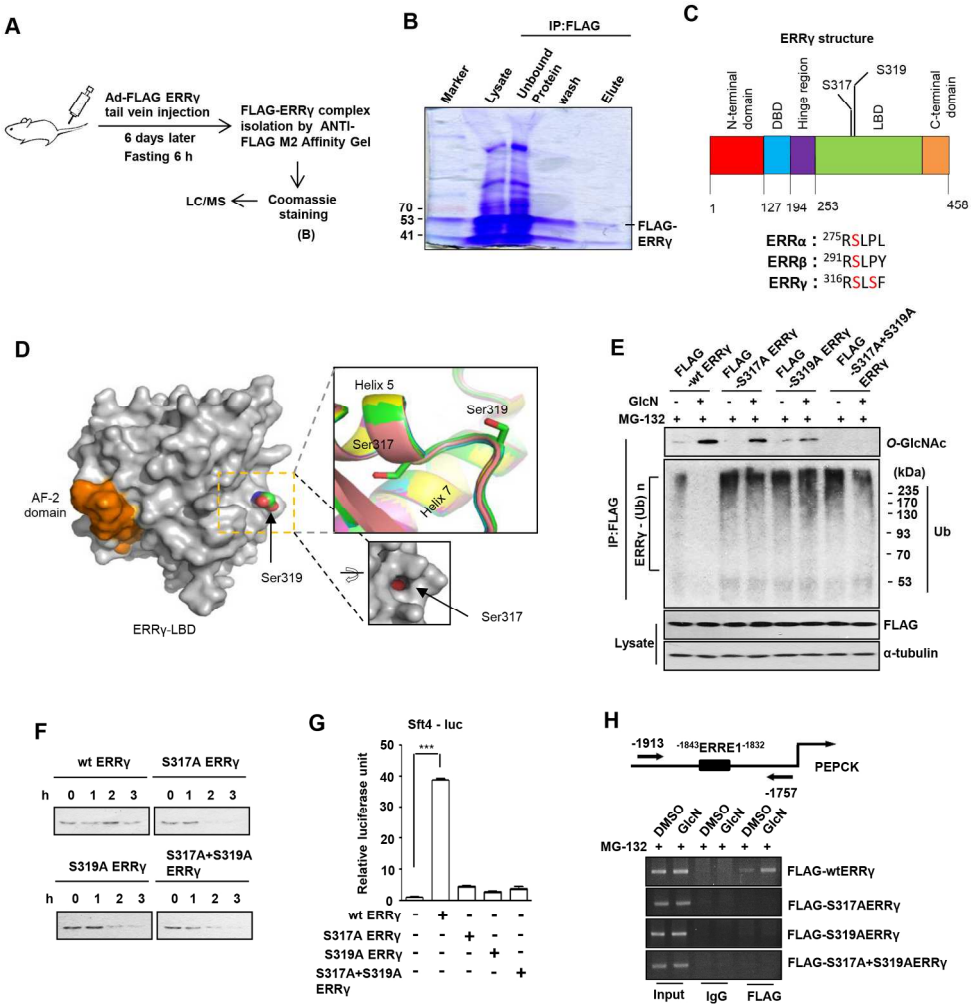

Figure 3
190x212mm (300 x 300 DPI)

Figure 4

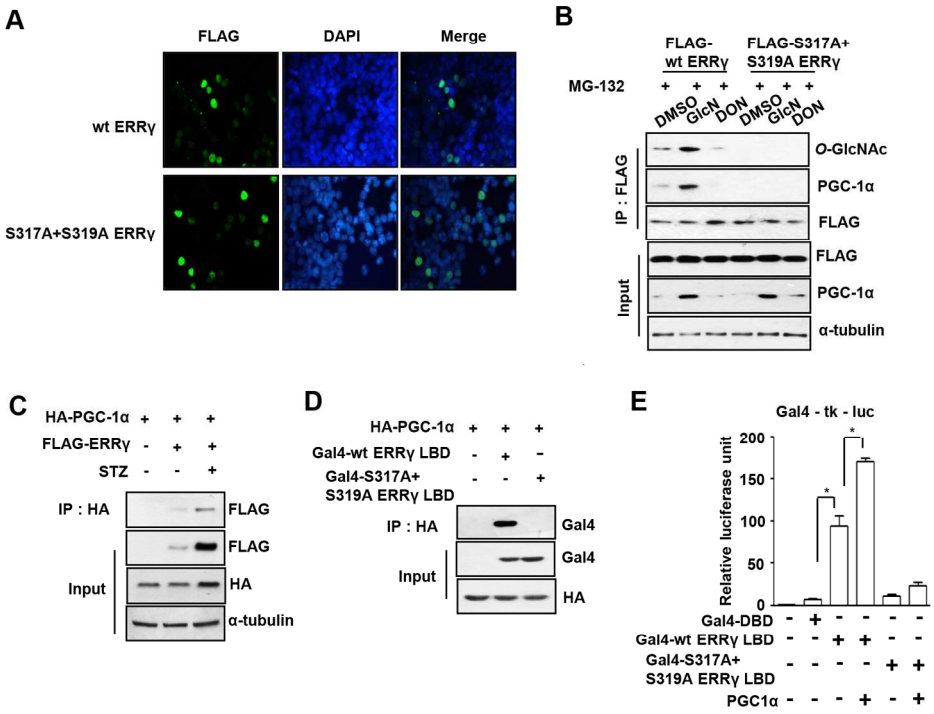

Figure 4
157x140mm (300 x 300 DPI)

Figure 5

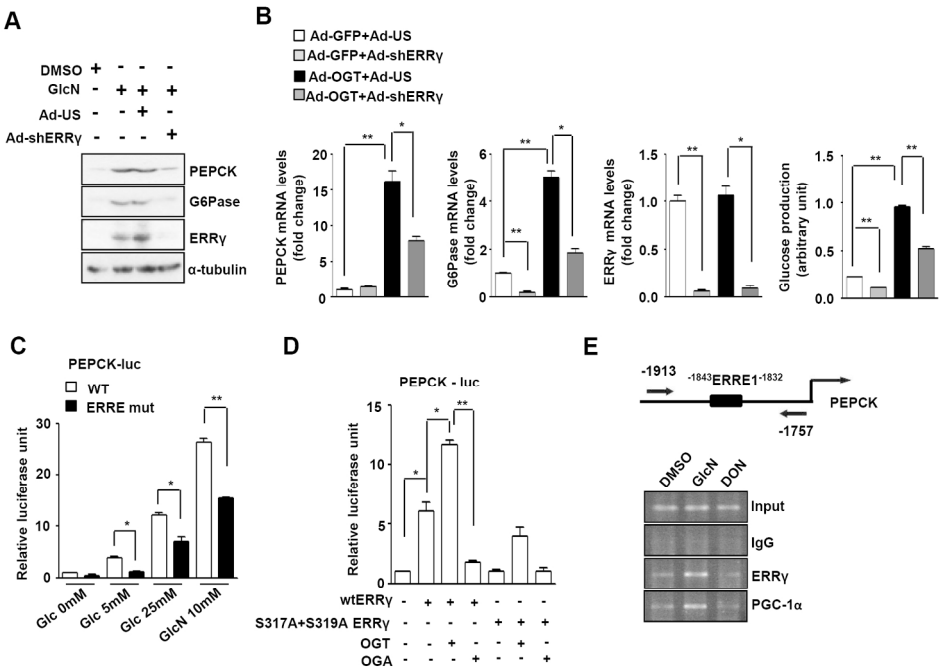

Figure 5
176x142mm (300 x 300 DPI)

Figure 6

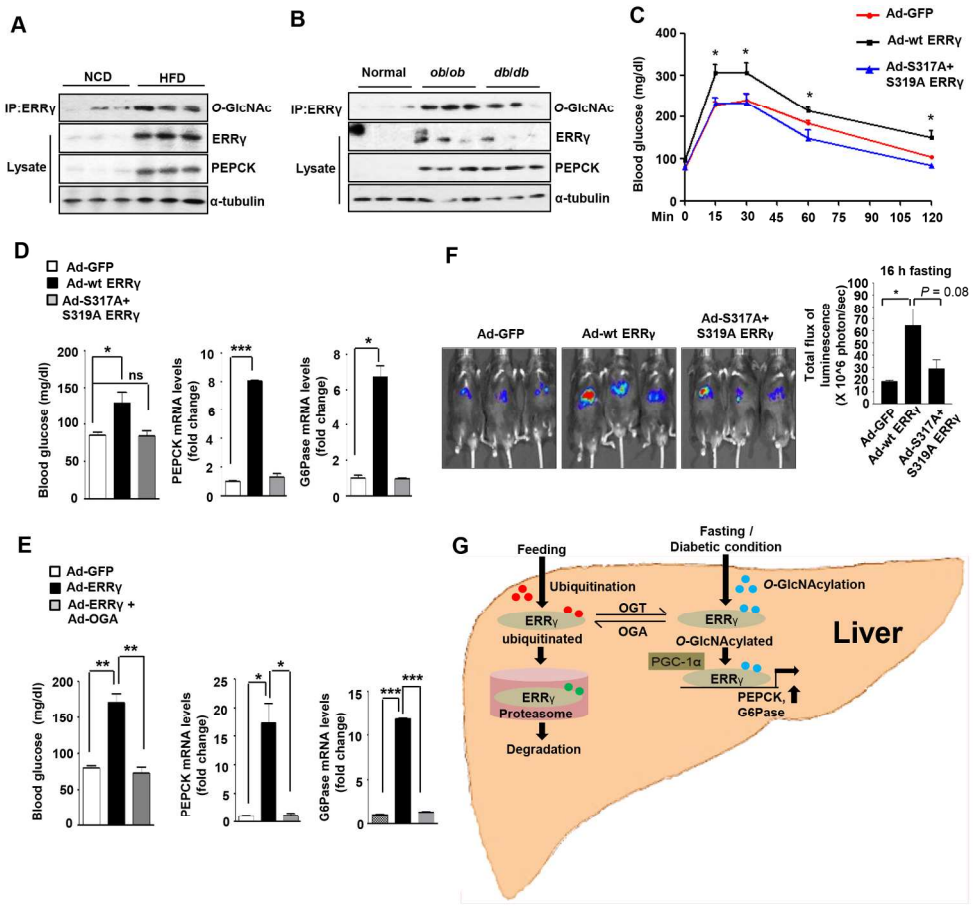

Figure 6
190x193mm (300 x 300 DPI)

Supplemental Information

O-GlcNAcylation of orphan nuclear receptor ERRγ promotes hepatic gluconeogenesis

Running title: *O*-GlcNAcylation of ERRγ

Jagannath Misra[1], Don-Kyu Kim[1], Yoon Seok Jung[1], Han Byeol Kim[2], Yong-Hoon Kim[3], Eun-Kyung Yoo[4], Byung Gyu Kim[5], Sunghoon Kim[6], In-Kyu Lee[4], Robert A. Harris[7], Jeong-Sun Kim[8], Chul-Ho Lee[3], Jin Won Cho[2] and Hueng-Sik Choi[1]*

[1]National Creative Research Initiatives Center for Nuclear Receptor Signals and Hormone Research Center, School of Biological Sciences and Technology, Chonnam National University, Gwangju 500-757, Republic of Korea. [2]Department of Integrated OMICS for Biomedical Science, Yonsei University, Seoul 120-749, Republic of Korea. [3]Korea Research Institute of Bioscience and Biotechnology, Daejeon 305-806, Republic of Korea. [4]Department of Internal Medicine, Kyungpook National University School of Medicine, Deagu 700-721, Republic of Korea. [5]Leading-edge Research Center for Drug Discovery and Development and Metabolic Disease, Kyungpook National University, Daegu 700-721, Korea. [6]Medicinal Bioconvergence Research Center Department of Molecular Medicine and Biopharmaceutical Sciences Graduate School of Convergence Science and Technology College of Pharmacy, Seoul National University, Seoul 151-742, Korea. [7]Department of Biochemistry and Molecular Biology, Indiana University School of Medicine and the Roudebush VA Medical Center, Indianapolis, Indiana 46202, United States of America. [8]Department of Chemistry and Institute of Basic Sciences, Chonnam National University, Gwangju 500-757, Republic of Korea.

CONTENTS

190x236mm (300 x 300 DPI)

FIGURE LEGENDS

Supplementary Figure 1. *O*-GlcNAcylation is affected by both glucosamine and high glucose levels. (A) AML12 cells were treated with DMSO or GlcN (10 mM) for 6 h as indicated. Immunoprecipitation with ERRγ antibody and western blot analyses with Ub, ERRγ and α-tubulin antibodies were performed. (B) HEK 293T cells were transfected with Sft4-luc along with the indicated plasmids followed by GlcN (10 mM) treatment for 6 h. (C) Liver tissue from C57BL/6 mice (n=5) fasted for different time points as indicated, was homogenized for immunoprecipitation with ERRγ antibody and immunoblot with OGT, OGA and α-tubulin antibodies. All of the samples were combined for western blot analyses. (D) Liver tissue from C57BL/6 mice (n=5) fasted for different time points as indicated, was homogenized for RNA isolation and qPCR analyses of total RNA. (E) Fasting blood glucose levels in C57BL/6 mice (n=5). (F) Fasting blood glucagon levels in C57BL/6 mice (n=5). (G) AML12 cells were incubated in 5 mM or 25 mM glucose media overnight followed by glucagon (100 nM) treatment for 6 h. Immunoprecipitation with ERRγ antibody and western blot analyses with *O*-GlcNAc, ERRγ and α-tubulin antibodies were performed as indicated. (H) AML12 cell were treated with GlcN or different doses of glucose for 6 h followed by ERRγ mRNA measurement by qPCR. NS, not significant. *p <0.05, **P <0.005 and ***<0.0005 using Student's t-test. Error bars show ± s.e.m.

Supplementary Figure 2. LC-MS/MS CID site mapping of the ERRγ *O*-GlcNAc modification site, Ser317. Sequence: SLSFEDELVYADDYIMDEDQSK, S1-HexNAc (203.07937 Da), M16-Oxidation (15.99492 Da) MS/MS: CID, Charge: +3, Monoisotopic m/z: 944.40265 Da (-1.41 mmu/-1.5 ppm), MH+: 2831.19339 Da, RT: 46.62 min, Identified with: SEQUEST (v1.13); XCorr: 2.61, Probability:3.23, Ions matched by search engine: 43/252

Fragment match tolerance used for search: 1.2 Da Fragments used for search: a-H2O; a-NH3; b; b-H2O; b-NH3; c; y; y-H2O; y-NH3; z+1

175x214mm (300 x 300 DPI)

Supplementary Figure 3. LC-MS/MS CID site mapping of the ERRγ *O*-GlcNAc modification site, Ser319. Sequence: SLSFEDELVYADDYIMDEDQSK, S3-HexNAc (203.07937 Da), M16-Oxidation (15.99492 Da), MS/MS: CID, Charge: +3, Monoisotopic m/z: 944.40356 Da (-0.5 mmu/-0.53 ppm), MH+: 2831.19614 Da, RT: 46.73 min, Identified with: SEQUEST (v1.13); XCorr:2.56, Probability:3.11, Ions matched by search engine: 39/208
Fragment match tolerance used for search: 1.2 Da ERRG #

Supplementary Figure 4. *O*-GlcNAcylation affects ERRγ protein stability and activity. (A) HEK 293T cells were transfected with plasmids encoding FLAG-wt ERRγ, FLAG-Ser317Ala ERRγ, FLAG-Ser319Ala ERRγ and FLAG-Ser317Ala+Ser319Ala ERRγ. At 24 h after transfection cells were treated with cycloheximide (CHX) (10 mg/mL) for the indicated times and FLAG-ERRγ levels were detected by immunoblot using FLAG and α-tubulin antibodies. (B) AML12 cell were treated with DMSO or GlcN or DON for 6 h followed by PGC-1α mRNA measurement by qPCR. NS, not significant. (C) HEK 293T cells were transfected with plasmids encoding FLAG-wt ERRγ, FLAG-Ser317Ala ERRγ, FLAG-Ser319Ala ERRγ, FLAG-Ser317Ala+Ser319Ala ERRγ and HA-PGC-1α. At 24 h post transfection cells were treated with MG-132 (10 μM) for 6 h followed by immunoprecipitation with HA antibody and immunoblot with FLAG, HA and α-tubulin antibodies. (D) HEK 293T cells were transfected with Gal4-tk-luc along with the indicated plasmids followed by GlcN (10 mM) treatment for 6 h. (E) Effectiveness of OGT overexpression was confirmed by western blot analyses. Mouse Primary hepatocytes were first infected with Ad-US or Ad-shERRγ followed by Ad-GFP or Ad-OGT infection as indicated. Total proteins were analyzed for the FLAG expression by immunoblot. (F) Liver tissue of C57BL/6 mice (n=3) fed with NCD or HFD was homogenized for RNA isolation and qPCR analyses of total RNA. (G) Effectiveness of ERRγ overexpression was confirmed by western blot analyses. Ad-GFP, Ad-wt ERRγ or Ad-Ser317Ala+Ser319Ala ERRγ was administered via tail-vein injection into C57BL/6 mice (n=5). Total proteins were isolated at day 7 after injection and analyzed for the FLAG expression by immunoblot. (H) Effect of OGA overexpression on ERRγ was examined by western blot analyses. Ad-GFP, Ad-wt ERRγ or Ad-wt ERRγ +Ad-OGA was administered via tail-vein injection into C57BL/6 mice (n=5). Total proteins were isolated at day 7 after injection and analyzed for ERRγ expression by immunoblot. *p <0.05, **P <0.005 and ***<0.0005 using Student's t-test. Error bars show ± s.e.m.

175x237mm (300 x 300 DPI)

Supplementary Figure 1

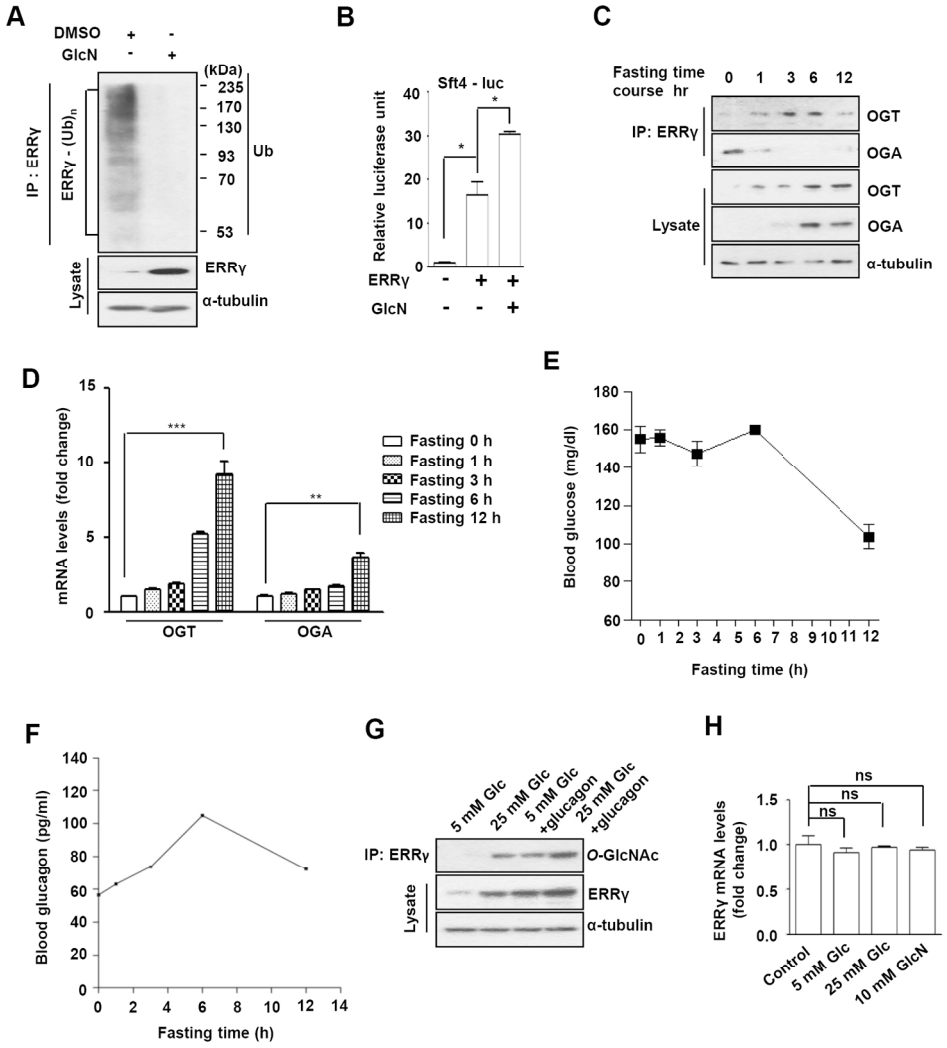

156x188mm (300 x 300 DPI)

Supplementary Figure 2

Serine 317 *O*-GlcNAcylation

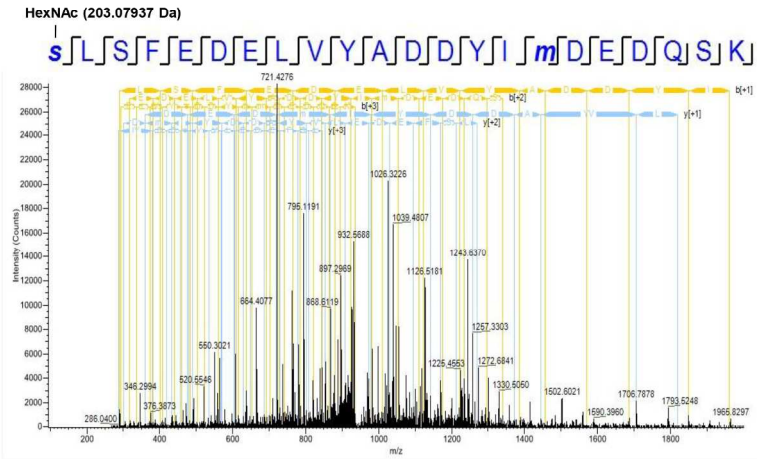

#1	b+	b2+	b3+	c+	c2+	c3+	Seq.	y+	y2+	y3+	z+1+	z+12+	z+13+	#2
1	291.11868	146.06298	97.71108	308.14523	154.57625	103.38659	S-HexNAc							22
2	404.20275	202.60501	135.40577	421.22930	211.11829	141.08128	L	2541.08623	1271.04675	847.70026	2526.07533	1263.54130	842.69663	21
3	491.23478	246.12103	164.41644	508.26133	254.63430	170.09196	S	2428.00216	1214.50472	810.00557	2412.99126	1206.99927	805.00194	20
4	638.30320	319.65524	213.43925	655.32975	328.16851	219.11477	F	2340.97013	1170.98870	780.99489	2325.95923	1163.48325	775.99126	19
5	767.34580	384.17654	256.45345	784.37235	392.68981	262.12897	E	2193.90171	1097.45449	731.97209	2178.89081	1089.94904	726.96845	18
6	882.37275	441.69001	294.79577	899.39930	450.20329	300.47128	D	2064.85911	1032.93319	688.95789	2049.84821	1025.42774	683.95425	17
7	1011.41535	506.21131	337.80997	1028.44190	514.72459	343.48548	E	1949.83216	975.41972	650.61557	1934.82126	967.91427	645.61194	16
8	1124.49942	562.75335	375.50466	1141.52597	571.26662	381.18017	L	1820.78956	910.89842	607.60137	1805.77866	903.39297	602.59774	15
9	1223.56784	612.28756	408.52746	1240.59439	620.80083	414.20298	V	1707.70549	854.35638	569.90668	1692.69459	846.85093	564.90305	14
10	1386.63116	693.81922	462.88190	1403.65771	702.33249	468.55742	Y	1608.63707	804.82217	536.88387	1593.62617	797.31672	531.88024	13
11	1457.66828	729.33778	486.56094	1474.69483	737.85105	492.23646	A	1445.57375	723.29051	482.52943	1430.56285	715.78506	477.52580	12
12	1572.69523	786.85125	524.90326	1589.72178	795.36453	530.57878	D	1374.53663	687.77195	458.85039	1359.52573	680.26650	453.84676	11
13	1687.72218	844.36473	563.24558	1704.74873	852.87800	568.92109	D	1259.50968	630.25848	420.50808	1244.49878	622.75303	415.50444	10
14	1850.78550	925.89639	617.60002	1867.81205	934.40966	623.27553	Y	1144.48273	572.74500	382.16576	1129.47183	565.23955	377.16213	9
15	1963.86957	982.43842	655.29471	1980.89612	990.95170	660.97022	I	981.41941	491.21334	327.81132	966.40851	483.70789	322.80769	8
16	2110.90498	1055.95613	704.30651	2127.93153	1064.46941	709.98203	M-Oxidation	868.33534	434.67131	290.11663	853.32444	427.16586	285.11300	7
17	2225.93193	1113.46961	742.64883	2242.95848	1121.98288	748.32435	D	721.29992	361.15360	241.10482	706.28902	353.64815	236.10119	6
18	2354.97453	1177.99091	785.66303	2372.00108	1186.50418	791.33855	E	606.27297	303.64012	202.76251	591.26207	296.13467	197.75888	5
19	2470.00148	1235.50438	824.00535	2487.02803	1244.01766	829.68086	D	477.23037	239.11882	159.74831	462.21947	231.61337	154.74468	4
20	2598.06006	1299.53367	866.69154	2615.08661	1308.04695	872.36706	Q	362.20342	181.60535	121.40599	347.19252	174.09990	116.40236	3
21	2685.09209	1343.04969	895.70222	2702.11864	1351.56296	901.37773	S	234.14484	117.57606	78.71980	219.13394	110.07061	73.71617	2
22							K	147.11281	74.06004	49.70912	132.10191	66.55459	44.70549	1

175x240mm (300 x 300 DPI)

Supplementary Figure 3

Serine 319 *O*-GlcNAcylation

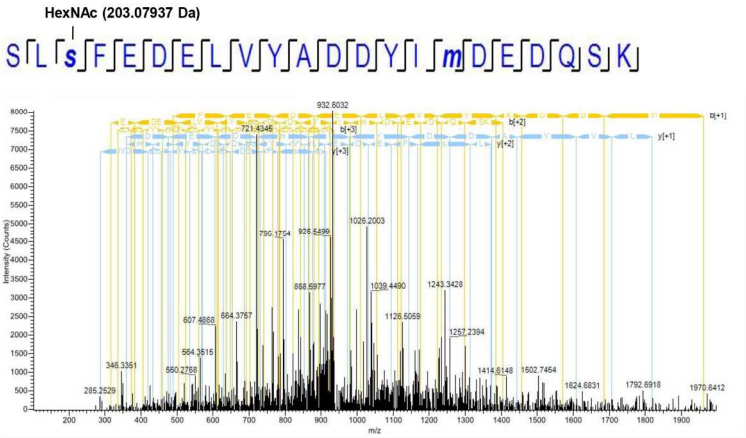

#1	b⁺	b²⁺	b³⁺	c⁺	c²⁺	c³⁺	Seq.	y⁺	y²⁺	y³⁺	z+1⁺	z+1²⁺	z+1³⁺	#2
1	88.03931	44.52329	30.01795	105.06586	53.03657	35.69347	S							22
2	201.12338	101.06533	67.71264	218.14993	109.57860	73.38816	L	2744.16560	1372.58644	915.39338	2729.15470	1365.08099	910.38975	21
3	491.23478	246.12103	164.41644	508.26133	254.63430	170.09196	S-HexNAc	2631.08153	1316.04440	877.69869	2616.07063	1308.53895	872.69506	20
4	638.30320	319.65524	213.43925	655.32975	328.16851	219.11477	F	2340.97013	1170.98870	780.99489	2325.95923	1163.48325	775.99126	19
5	767.34580	384.17654	256.45345	784.37235	392.68981	262.12897	E	2193.90171	1097.45449	731.97209	2178.89081	1089.94904	726.96845	18
6	882.37275	441.69001	294.79577	899.39930	450.20329	300.47128	D	2064.85911	1032.93319	688.95789	2049.84821	1025.42774	683.95425	17
7	1011.41535	506.21131	337.80997	1028.44190	514.72459	343.48548	E	1949.83216	975.41972	650.61557	1934.82126	967.91427	645.61194	16
8	1124.49942	562.75335	375.50466	1141.52597	571.26662	381.18017	L	1820.78956	910.89842	607.60137	1805.77866	903.39297	602.59774	15
9	1223.56784	612.28756	408.52746	1240.59439	620.80083	414.20298	V	1707.70549	854.35638	569.90668	1692.69459	846.85093	564.90305	14
10	1386.63116	693.81922	462.88190	1403.65771	702.33249	468.55742	Y	1608.63707	804.82217	536.88387	1593.62617	797.31672	531.88024	13
11	1457.66828	729.33778	486.56094	1474.69483	737.85105	492.23646	A	1445.57375	723.29051	482.52943	1430.56285	715.78506	477.52580	12
12	1572.69523	786.85125	524.90326	1589.72178	795.36453	530.57878	D	1374.53663	687.77195	458.85039	1359.52573	680.26650	453.84676	11
13	1687.72218	844.36473	563.24558	1704.74873	852.87800	568.92109	D	1259.50968	630.25848	420.50808	1244.49878	622.75303	415.50444	10
14	1850.78550	925.89639	617.60002	1867.81205	934.40966	623.27553	Y	1144.48273	572.74500	382.16576	1129.47183	565.23955	377.16213	9
15	1963.86957	982.43842	655.29471	1980.89612	990.95170	660.97022	I	981.41941	491.21334	327.81132	966.40851	483.70789	322.80769	8
16	2110.90498	1055.95613	704.30651	2127.93153	1064.46941	709.98203	M-Oxidation	868.33534	434.67131	290.11663	853.32444	427.16586	285.11300	7
17	2225.93193	1113.46961	742.64883	2242.95848	1121.98288	748.32435	D	721.29992	361.15360	241.10482	706.28902	353.64815	236.10119	6
18	2354.97453	1177.99091	785.66303	2372.00108	1186.50418	791.33855	E	606.27297	303.64012	202.76251	591.26207	296.13467	197.75888	5
19	2470.00148	1235.50438	824.00535	2487.02803	1244.01766	829.68086	D	477.23037	239.11882	159.74831	462.21947	231.61337	154.74468	4
20	2598.06006	1299.53367	866.69154	2615.08661	1308.04695	872.36706	Q	362.20342	181.60535	121.40599	347.19252	174.09990	116.40236	3
21	2685.09209	1343.04969	895.70222	2702.11864	1351.56296	901.37773	S	234.14484	117.57606	78.71980	219.13394	110.07061	73.71617	2
22							K	147.11281	74.06004	49.70912	132.10191	66.55459	44.70549	1

174x241mm (300 x 300 DPI)

Supplementary Figure 4

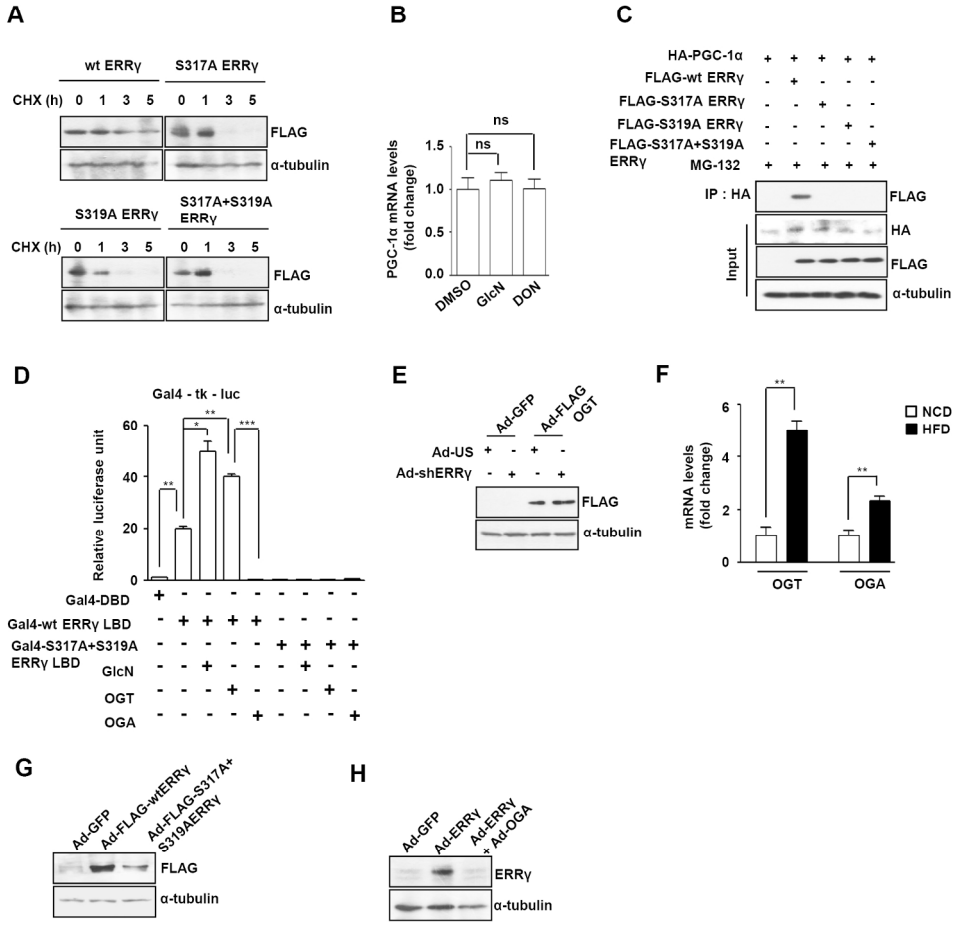

177x185mm (300 x 300 DPI)